AD-750 540

CODA SUPPRESSION CAPABILITIES OF THE BEAM AND MIXED-SIGNAL PROCESSOR

T. J. Cohen

Teledyne Geotech

Prepared for:

Advanced Research Projects Agency

30 August 1972

DISTRIBUTED BY:

National Technical Information Service
U. S. DEPARTMENT OF COMMERCE
5285 Port Royal Road, Springfield Va. 22151

BEST
AVAILABLE COPY

AD750540

298

... contributing to man's understanding of the environment world

DDC
RECEIVED
OCT 12 1972

CODA SUPPRESSION CAPABILITIES OF THE BEAM AND MIXED-SIGNAL PROCESSOR

T.J. COHEN

SEISMIC DATA LABORATORY

30 AUGUST 1972

Prepared for
AIR FORCE TECHNICAL APPLICATIONS CENTER
Washington, D.C.

Under
Project VELA UNIFORM

Sponsored by
ADVANCED RESEARCH PROJECTS AGENCY
Nuclear Monitoring Research Office
ARPA Order No. 1714

Reproduced by
NATIONAL TECHNICAL
INFORMATION SERVICE
U.S. Department of Commerce
Springfield VA 22151

TELEDYNE GEOTECH
ALEXANDRIA LABORATORIES

APPROVED FOR PUBLIC RELEASE; DISTRIBUTION UNLIMITED.

d

Unclassified
Security Classification

DOCUMENT CONTROL DATA - R&D

(Security classification of title, body of abstract and indexing annotation must be entered when the overall report is classified)

1 ORIGINATING ACTIVITY (Corporate author)
Teledyne Geotech
Alexandria, Virginia

2a REPORT SECURITY CLASSIFICATION
Unclassified

2b GROUP

3 REPORT TITLE
CODA SUPPRESSION CAPABILITIES OF THE BEAM AND MIXED-SIGNAL PROCESSOR

4 DESCRIPTIVE NOTES (Type of report and inclusive dates)
Scientific

5 AUTHOR(S) (Last name, first name, initial)
Cohen, T.J.

6 REPORT DATE	7a TOTAL NO. OF PAGES	7b NO OF REFS
30 August 1972	65	2

8a CONTRACT OR GRANT NO.	9a ORIGINATOR'S REPORT NUMBER(S)
F33657-72-C-0009 b PROJECT NO VELA T/2706 c ARPA Order No. 1714 d ARPA Program Code No. 2F-10	298 9b. OTHER REPORT NO(S) (Any other numbers that may be assigned this report)

10 AVAILABILITY/LIMITATION NOTICES
APPROVED FOR PUBLIC RELEASE; DISTRIBUTION UNLIMITED.

11 SUPPLEMENTARY NOTES	12 SPONSORING MILITARY ACTIVITY
	Advanced Research Projects Agency Nuclear Monitoring Research Office Washington, D.C.

13 ABSTRACT

Using 7- and 19-element subarrays at TFO we compare the relative abilities of the beam and a mixed-signal processor to attenuate P-wave codas. P-wave signals from various earthquakes are time-shifted to simulate arrivals from different azimuths and 60° distance. These signals are assumed to mask an explosion detonated at Semipalatinsk, about 96° distance from TFO. The analysis consists of determining how much of signal 1 (the earthquake) leaks into our estimate of signal 2 (the event being masked). Because the beam and mixed-signal processor are linear processors, signal 2 need not actually be present; we need only determine how much of signal 1 is present in our estimate of signal 2. The coda attenuation capability of the mixed-signal processor is found to exceed that of the beam. Up to 14 db improvement over the beam is obtained, although improvement is generally on the order of 3 to 5 db for both subarrays. A nominal value of 18 db is representative of the maximum coda attenuation obtained using the mixed signal processor and the 19-element subarray; for the 7-element subarray, maximum attenuation is roughly 14 db. Coda attenuation obtained using the 7-element subarray and the mixed-signal processor is comparable to that obtained using the 19-element subarray and the beam. Representative TFO coda-attenuation curves for the mixed-signal processor are: 19 elements:

$$\rho = \frac{5.74X + 0.91X^2}{1.0 + 0.31X + 0.043X^2} \text{ db}$$

7 elements:

$$\rho = \frac{2.21X + 0.69X^2}{1.0 + 0.53X + 0.005X^2} \text{ db}$$

where

$$X = \left| \left(\frac{\partial \vec{t}}{\partial \Delta}\right)_1 - \left(\frac{\partial \vec{t}}{\partial \Delta}\right)_2 \right|$$

For X small, the mixed-signal processor is six times more sensitive to changes in X than is the beam. Preliminary results suggest that when the difference in the ray parameter vectors is small, a large-aperture array and the mixed-signal processor are required for significant coda attenuation (~9 db).

14 KEY WORDS
Beamforming
Mixed-Signal Processing
Coda Suppression

Unclassified
Security Classification

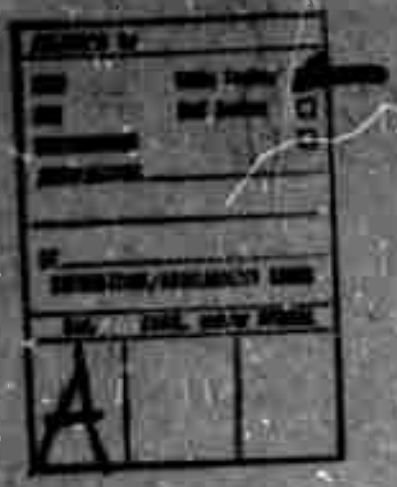

Neither the Advanced Research Projects Agency nor the Air Force Technical Applications Center will be responsible for information contained herein which has been supplied by other organizations or contractors, and this document is subject to later revision as may be necessary. The views and conclusions presented are those of the authors and should not be interpreted as necessarily representing the official policies, either expressed or implied, of the Advanced Research Projects Agency, the Air Force Technical Applications Center, or the U S Government.

CODA SUPPRESSION CAPABILITIES OF THE
BEAM AND MIXED-SIGNAL PROCESSOR

SEISMIC DATA LABORATORY REPORT NO. 298

AFTAC Project No.:	VELA T/2706
Project Title:	Seismic Data Laboratory
ARPA Order No.:	1714
ARPA Program Code No.:	2F-10
Name of Contractor:	TELEDYNE GEOTECH
Contract No.:	F33657-72-C-0009
Date of Contract:	01 July 1971
Amount of Contract:	$ 1,736,000
Contract Expiration Date:	31 October 1972
Project Manager:	Robert R. Blandford (703) 836-3882

P. O. Box 334, Alexandria, Virginia 22314

APPROVED FOR PUBLIC RELEASE; DISTRIBUTION UNLIMITED.

TABLE OF CONTENTS

	Page No.
ABSTRACT	
INTRODUCTION	1
SIGNAL ANALYSIS THEORY	3
DATA ANALYSIS	6
RESULTS	9
CONCLUSIONS	15
REFERENCES	17
ACKNOWLEDGEMENTS	18

LIST OF FIGURES

Figure Title	Figure No.
Least-square technique for estimation of one signal in presence of another (example).	1
Geographical location of TFO.	2
Array configuration for TFO.	3
Seismograms for the Easter Island event.	4
Seismograms for the Fiji Islands event.	5
Seismograms for the Fox Islands event.	6
Seismograms for the Hokkaido event.	7
Seismograms for the Tonga Islands event.	8
Coda attenuation, 19-element subarray, Easter Island event, seismograms bandpass filtered with 3 db points at 0.4 and 3.0 Hz.	9
Coda attenuation, 7-element subarray, Easter Island event, seismograms bandpass filtered with 3 db points at 0.4 and 3.0 Hz.	10
Coda attenuation, 19-element subarray, Fiji Islands event, seismograms bandpass filtered with 3 db points at 0.4 and 3.0 Hz.	11
Coda attenuation, 7-element subarray, Fiji Islands event, seismograms bandpass filtered with 3 db points at 0.4 and 3.0 Hz.	12
Coda attenuation, 19-element subarray, Fox Islands event, seismograms bandpass filtered with 3 db points at 0.4 and 3.0 Hz.	13
Coda attenuation, 7-element subarray, Fox Islands event, seismograms bandpass filtered with 3 db points at 0.4 and 3.0 Hz.	14

LIST OF FIGURES (Cont'd.)

Figure Title	Figure No.
Coda attenuation, 19-element subarray, Hokkaido event, seismograms bandpass filtered with 3 db points at 0.4 and 3.0 Hz.	15
Coda attenuation, 7-element subarray, Hokkaido event, seismograms bandpass filtered with 3 db points at 0.4 and 3.0 Hz.	16
Coda attenuation, 19-element subarray, Tonga Island event, seismograms bandpass filtered with 3 db points at 0.4 and 3.0 Hz.	17
Coda attenuation, 7-element subarray, Tonga Island event, seismograms bandpass filtered with 3 db points at 0.4 and 3.0 Hz.	18
Coda attenuation, 19-element subarray, Fox Islands event, seismograms bandpass filtered with 3 db points at 0.4 and 3.0 Hz.	19
Coda attenuation, 7-element subarray, Fox Islands event, seismograms bandpass filtered with 3 db points at 0.4 and 3.0 Hz.	20
Coda attenuation, 19-element subarray, Tonga Islands event, seismograms bandpass filtered with 3db points at 0.8 and 2.0Hz.	21
Coda attenuation, 7-element subarray, Tonga Islands event, seismograms bandpass filtered with 3db points at 0.8 and 2.0Hz.	22
Average coda attenuation, 19-element subarray.	23
Average coda attenuation, 7-element subarray.	24
Attenuation as a function of the difference in ray parameters, 19-element subarray, beam.	25

LIST OF FIGURES (Cont'd.)

Figure Title	Figure No.
Attenuation as a function of the difference in ray parameters, 19-element subarray, mixed-signal processor.	26
Attenuation as a function of the difference in ray parameters, 7-element subarray, beam.	27
Attenuation as a function of the difference in ray parameters. 7-element subarray, mixed-signal processor.	28
Coda attenuation, 19-element subarray, Fox Islands event, seismograms bandpass filtered with 3 db points at 0.4 and 3.0 Hz. (Signal 2 from Tonga Islands).	29
Coda attenuation, 7-element subarray, Fox Islands event, seismograms bandpass filtered with 3 db points at 0.4 and 3.0 Hz. (Signal 2 from Tonga Islands).	30
Comparison of coda attenuation figures, Easter Island event, 19-element subarray and wide-aperture 7-element subarray.	31
Comparison of coda attenuation figures, Easter Island event, small-aperture 7-element subarray and wide-aperture 7-element subarray.	

LIST OF TABLES

Table Title	Table No.
Earthquake Source Data	I
Coordinates of TFO Instruments	II
Coda Attenuation Parameters	III
Coda Attenuation Parameters	IV
Coda Attenuation Parameters	V
Comparison of Coda Attenuation Capabilities	VI

INTRODUCTION

The number of opportunities for masking the signals from an explosion in the coda of an earthquake depends critically on the amplitude-time characteristics of the earthquake coda at various stations within a monitoring network. When coda are suppressed, the time window available for masking is reduced, and so, correspondingly, are the number of testing opportunities.

Given that the explosion is to be masked in an earthquake which may occur anywhere on the earth, the classical method for coda suppression is to beam on the suspected test site. For a 19-element subarray such as the innermost elements at TFO, beamforming might be expected to yield coda suppression on the order of 13 db. This attenuation figure, however, is based on a random noise model. In reality the noise we are trying to suppress is a teleseismic signal propagating across the array. We therefore expect coda attenuation to be a function of the difference between the apparent velocities across the array for the two interfering signals, as well as of the angular separation between the event epicenters. Further, because a mixed-signal processor would take account of a second signal's presence, we expect, a priori, that this processor would equal or exceed the coda attenuation capability of the beam.

In this report we investigate the coda suppression capabilities of the beam and mixed-signal processor using 7- and 19-element subarrays at TFO. The analysis consists of determining how much of signal 1

(the earthquake) "leaks" into our estimate of signal 2 (the event to be masked). We would like to perform this analysis using two overlapping signals actually recorded at TFO. However, this would not yield acceptable results because we would not know the true waveforms of either signal. Alternatively, we could add two signals together. In this case, we would have to form the beam of the signal from the explosion site and subtract it from the beam of the composite seismograms in order to determine the residual signal leaking through from the earthquake signal. This method would have to be employed if nonlinear processes were involved. Fortunately, both the beam and mixed-signal processor involve linear processes. Thus, signal 2 need not be present in the seismograms analyzed because we only seek to determine how much of signal 1 is present in our estimate of signal 2. We proceed as follows: we simply simulate the arrival of an earthquake at various azimuths and at a fixed distance of 60° from TFO, and estimate the signal leakage for a fixed test site. The ratio of the root mean square (rms) power for the leakage signal to the average rms power of the earthquake arrivals is then defined as the coda attenuation.

We analyzed the seismograms for five real events, time-shifted them to produce simulated arrivals, and studied the coda attenuation for a variety of signal waveform types.

Consider the following representation for a collection of signals:

$$y_j(t) = \sum_{u=-\infty}^{\infty} \sum_{k=1}^{p} x_{jk}(t-u)s_k(u) + n_j(t) \qquad (1)$$

where

$y_j(t)$, $j = 1,\ldots, n$ is the collection of N observed series;

$s(t)$, $k = 1,\ldots, p$ is the collection of signals to be estimated

$x_{jk}(t) = \delta(t-T_{jk})$[where $\delta(t) = 1$ for $t = 0$, zero otherwise];

and

$n_j(t)$ is the noise on the j'th channel.

Further, assume that the signals can be estimated by a linear estimates of the type:

$$\hat{s}_k(t) = \sum_{j=1}^{n} \int_{-\infty}^{\infty} h_{kj}(\tau)y_j(t-\tau)d\tau \qquad (2)$$

where $h_{kj}(t)$ is a p x n matrix of filter functions to be determined.

Using the above, it can be shown (Dean et al., 1968) that in the frequency domain the matrix of filter coefficients $H(\omega)$ which produces the best linear unbiased estimates of the $s_k(t)$ is given by

$$H(\omega) = (X^*\sum^{-1}X)^{-1}X^*\sum^{-1}(\omega) \tag{3}$$

where $\sum \equiv \{\sigma^2_{kj}(\omega)\}$, an n x n matrix of spectra and cross-spectra at frequency ω. By calculating $H(\omega)$ at each frequency and then transforming back into time, one need only convolve the filters obtained with the $y_j(t)$ to produce the signal estimates $\hat{s}_k(t)$. For a single signal (k=1) in uncorrelated noise, $\hat{s}_1(t)$ is the beam.

A rough estimate of the coda suppression capabilities of the beam and mixed signal processor may be had by analyzing the results shown in Figure 1 (Shumway, 1972). Here two signals recorded separately are superimposed to simulate interfering arrivals. Signal 2, which in our case represents the explosion, is shown arriving first. This signal is actually a Tonga Islands earthquake. Signal 1, the masking earthquake, is a Fox Islands earthquake. Normalizing all measurements to the second (undisturbed) cycle of the Tonga Islands event, we see that the leakage of signal 1 into the beam at point (B) in the figure is only 5 db down from the unprocessed signal shown at (A), while the mixed signal processor has reduced signal 1 at (C) by 13 db compared to the signal at (A). Thus, in this example, leakage of

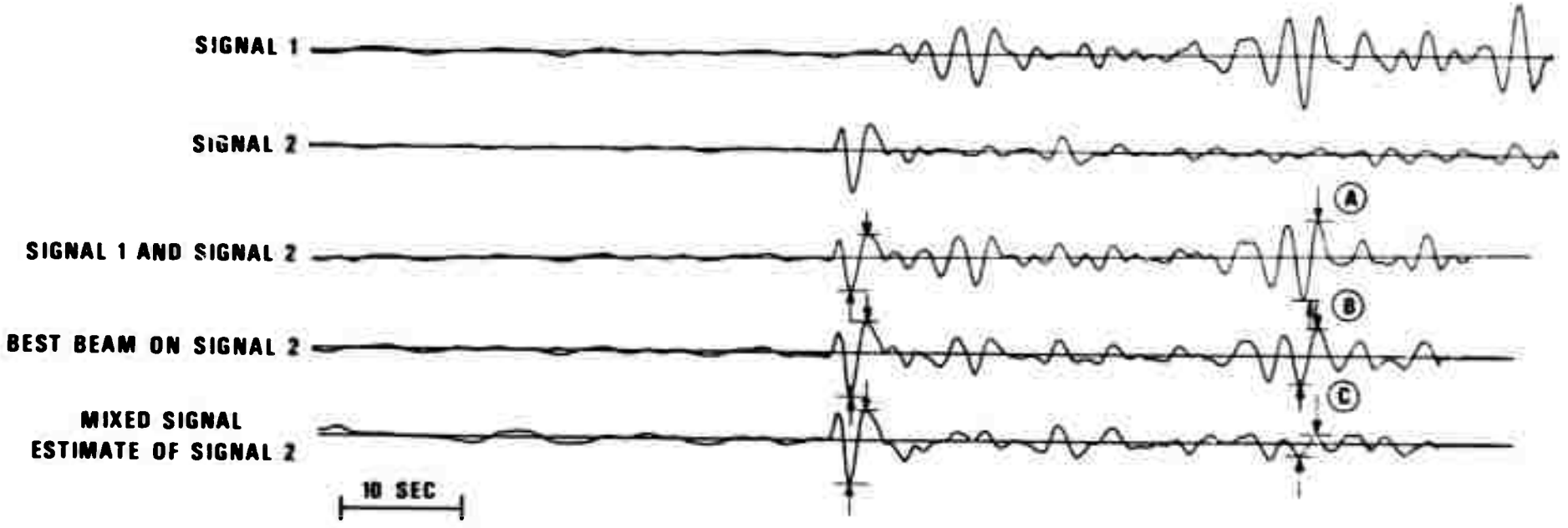

Figure 1. Least-square technique for estimation of one signal in presence of another (example). After Shumway (1972).

signal 1 into our mixed signal estimate is reduced by 8 db over the leakage observed in the beam trace.

DATA ANALYSIS

A suite of five earthquakes (Table I) recorded at TFO (Figures 2 and 3, Table II) provides the data base for this study. The filtered traces (the filter has 0.4 and 3.0 Hz 3 db points) are shown in Figures 4 through 8. The 7- and 19-element subarrays to be examined consist of elements Z1 through Z7, and of Z1 through Z19, respectively. The first arrivals for all the events exhibit signal-to-noise ratios greater than 20 db. Signals with high signal-to-noise ratios are required to insure that background noise does not enter into the computations.

For a given event and subarray, the analysis procedure is as follows: the onset of the event (or other common point within the first second of onset) is picked on each channel. With these common picks as reference points, the traces are shifted relative to one another to simulate the arrival of the event from a given distance and azimuth.

Using the shifted traces, the beam and mixed-signal estimates are then computed for a signal presumed to originate at a selected test site. These signal estimates represent the leakage from signal 1 (the earthquake) into the estimates for signal 2 (the explosion). The power for the leakage signals, when ratioed to the averaged power for the earthquake arrivals, yields a set of coda attenuation figures for the two processors. That is, let $\bar{R}$ be a measure of the average rms input signal power:

TABLE I

Earthquake Source Data

REGION	DATE	LATITUDE	LONGITUDE	DEPTH (km)	m_b	ORIGIN TIME			DISTANCE TO TFO
Easter Island	09 Sep 69	4.4°S	105.9°W	33	5.2	15	23	10.8	38.4°
Fiji Islands	01 Aug 69	23.4°S	177.5°W	189	5.0	12	05	34.6	84.5°
Fox Islands	24 Aug 69	52.5°N	168.6°W	33	5.2	00	46	14.6	44.7°
Hokkaido	20 Jun 69	40.8°N	142.1°E	67	5.4	15	37	50.2	79.3°
Tonga Islands	22 Jul 69	18.1°S	172.5°W	30	5.4	13	48	36.5	78.0°

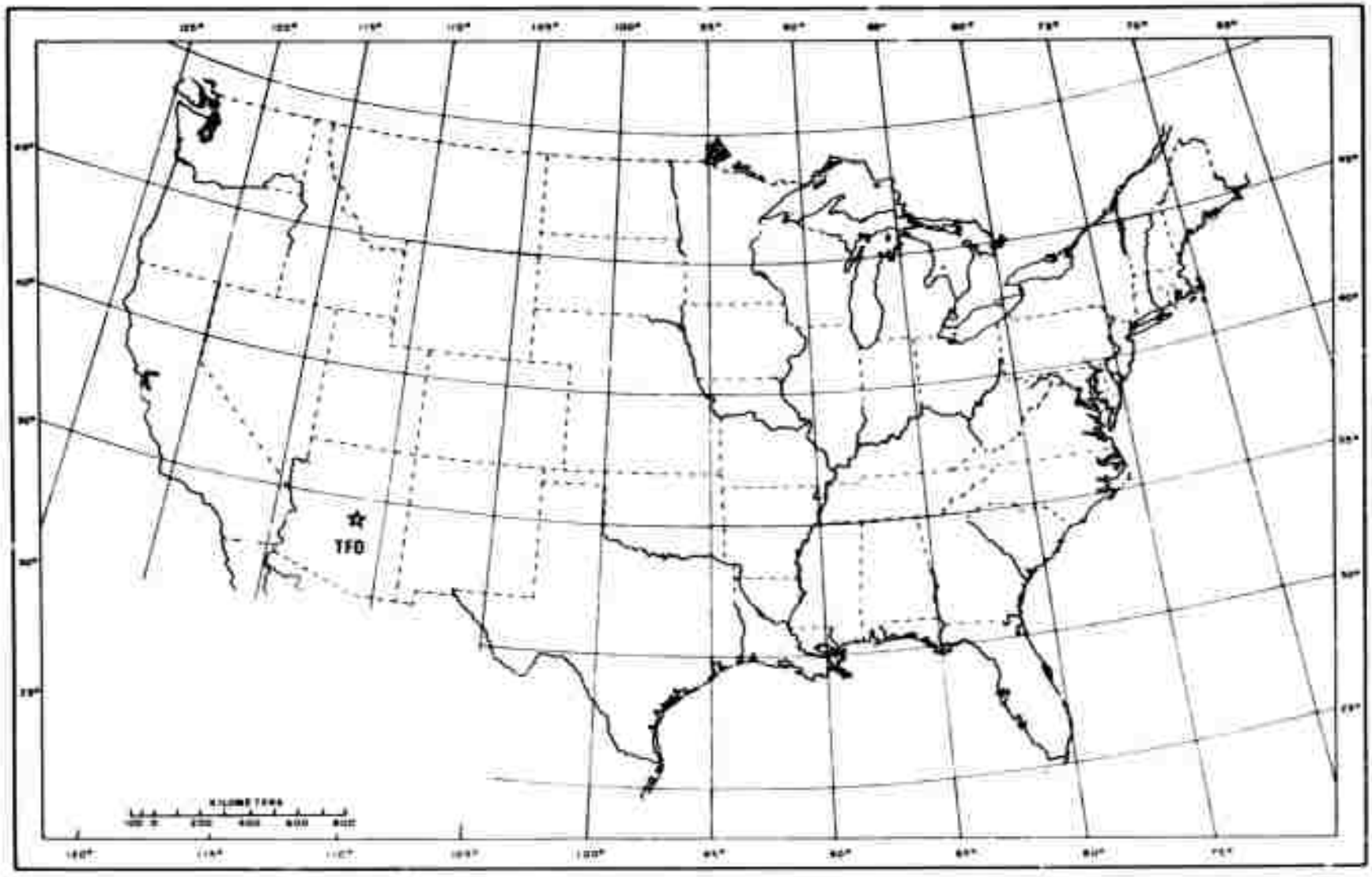

Figure 2. Geographical location of TFO.

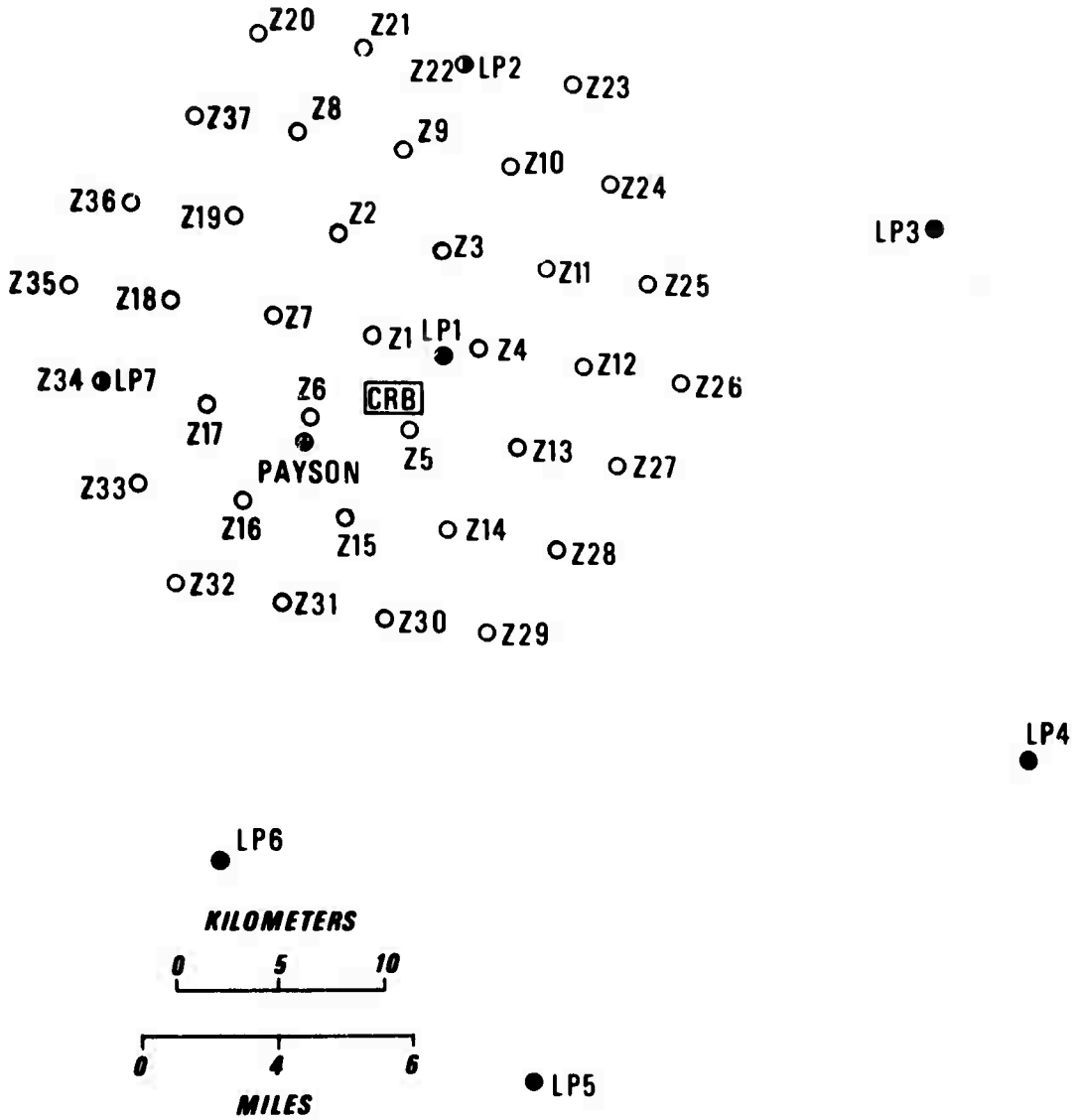

(1) THE ○ CIRCLES LABELED Z1 THROUGH Z37 ARE CENTERED ON THE 37 SHORT PERIOD SEISMOMETER LOCATIONS.

(2) THE ● CIRCLES LABELED LP1 THROUGH LP7 ARE CENTERED ON THE 7 THREE -COMPONENT LONG PERIOD SEISMOMETERS.

(3) THE CRB IS THE CENTRAL RECORDING BUILDING.

Figure 3. Array configuration for TFO.

TABLE II

Coordinates of TFO Instruments

Z1 - Z19

SHORT PERIOD

	LATITUDE	LONGITUDE	ELEVATION (Meters)
Z-1	34 16 42.3300N	111 18 12.2560W	1615.42
Z-2	34 19 14.1190N	111 19 26.6720W	1489.75
Z-3	34 18 42.5760N	111 16 56.0730W	1515.3
Z-4	34 16 13.8910N	111 14 56.7380W	1474.6
Z-5	34 14 10.2220N	111 17 2.2670W	1491.9
Z-6	34 14 55.6970N	111 20 7.0030W	1509.4
Z-7	34 17 9.1830N	111 21 24.5490W	1403.2
Z-8	34 21 42.2900N	111 20 23.5360W	1805.4
Z-9	34 21 10.0020N	111 17 12.9640W	1569.4
Z-10	34 20 52.2090N	111 14 4.9130W	1658.5
Z-11	34 18 4.8650N	111 12 23.8630W	1904.9
Z-12	34 15 49.5070N	111 11 44.7380W	1528.29
Z-13	34 13 48.4020N	111 13 48.3160W	1513.74
Z-14	34 11 41.4430N	111 16 30.2940W	1534.0
Z-15	34 12 8.0760N	111 19 8.4440W	1487.4
Z-16	34 12 32.0810N	111 22 13.9550W	1462.9
Z-17	34 15 3.9540N	111 23 28.2740W	1426.4
Z-18	34 17 40.8760N	111 24 39.9550W	1664.9
Z-19	34 19 39.8540N	111 22 32.4010W	1588.55

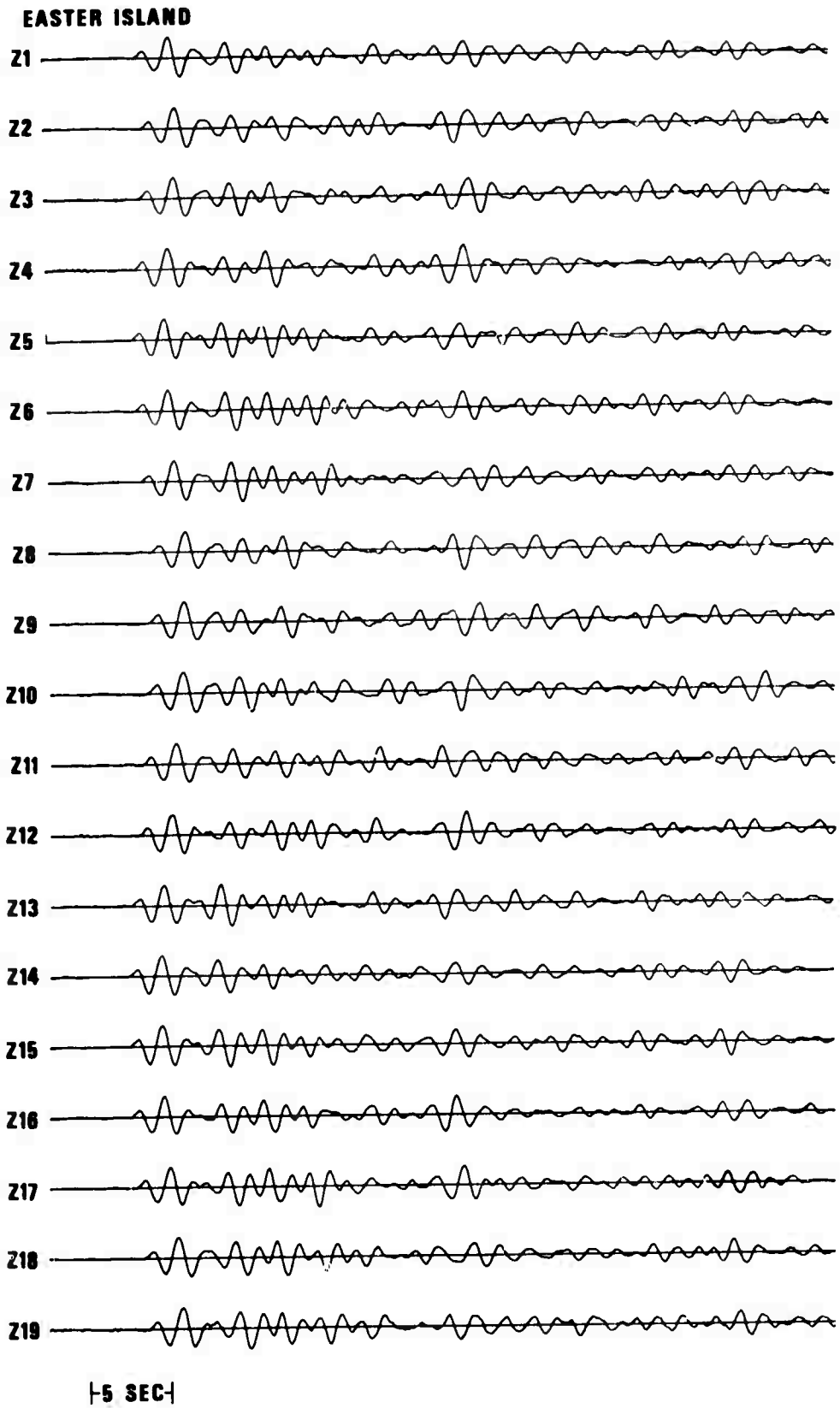

Figure 4. Seismograms for the Easter Island event.

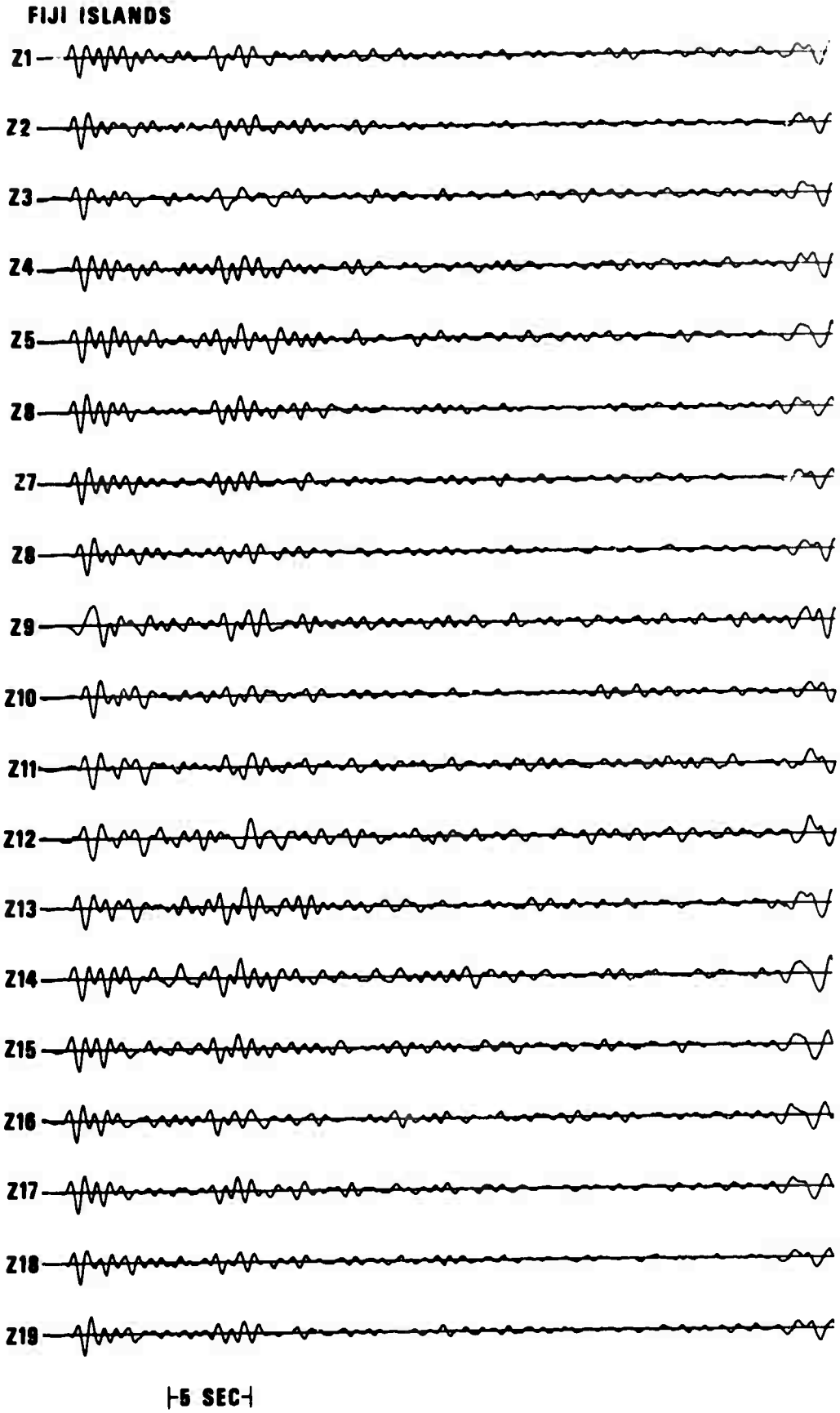

Figure 5. Seismograms for the Fiji Islands event.

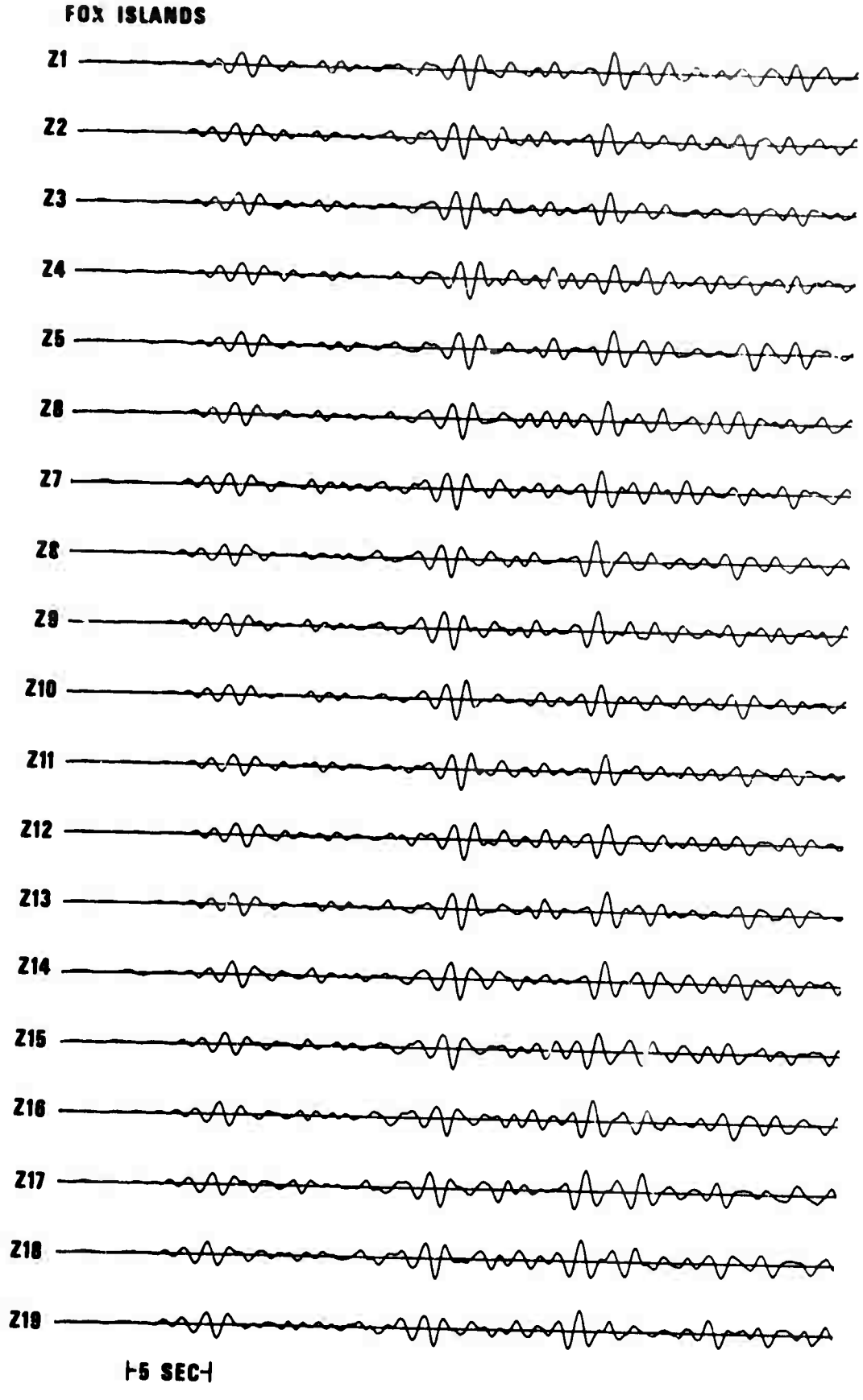

Figure 6. Seismograms for the Fox Islands event.

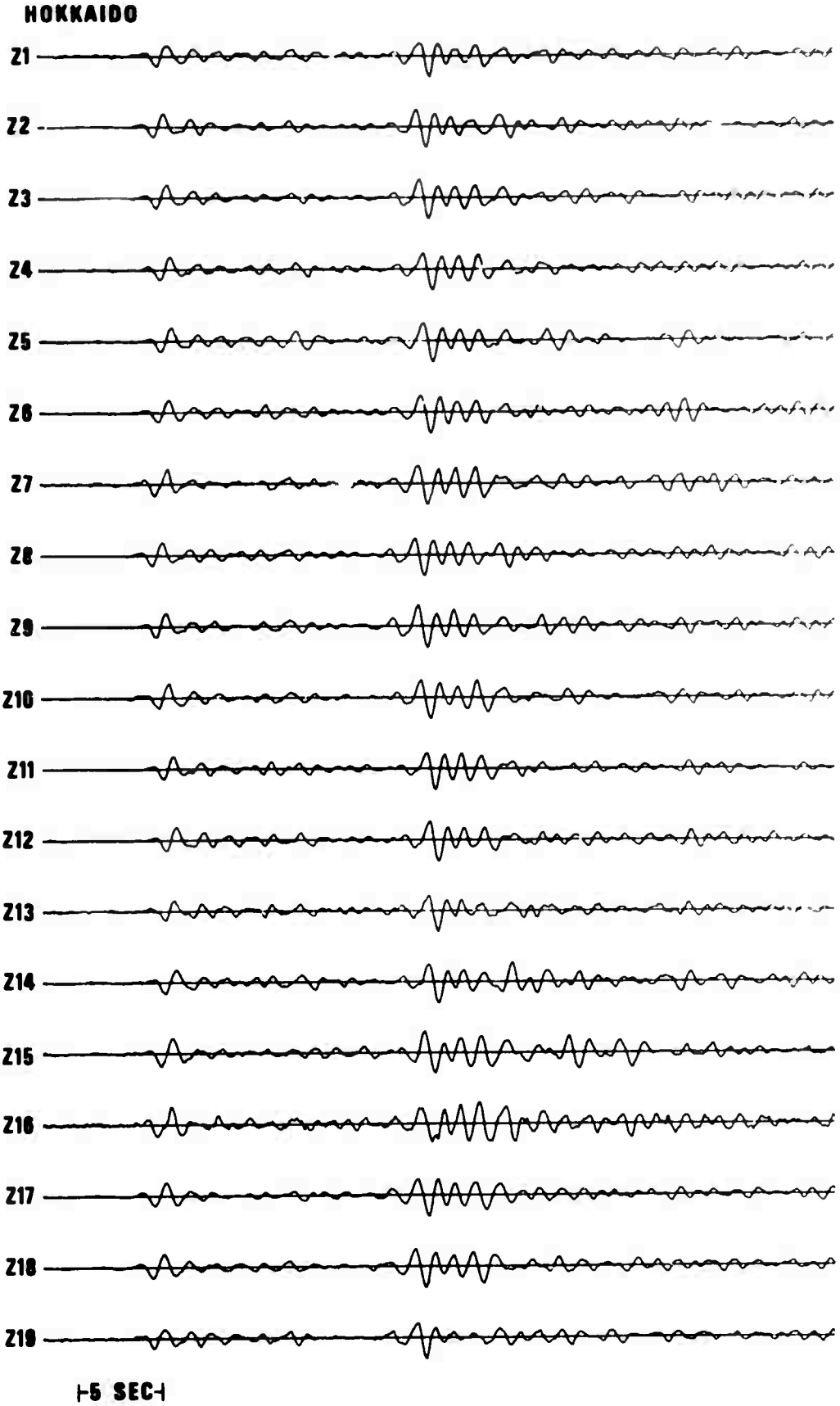

Figure 7. Seismograms for the Hokkaido event.

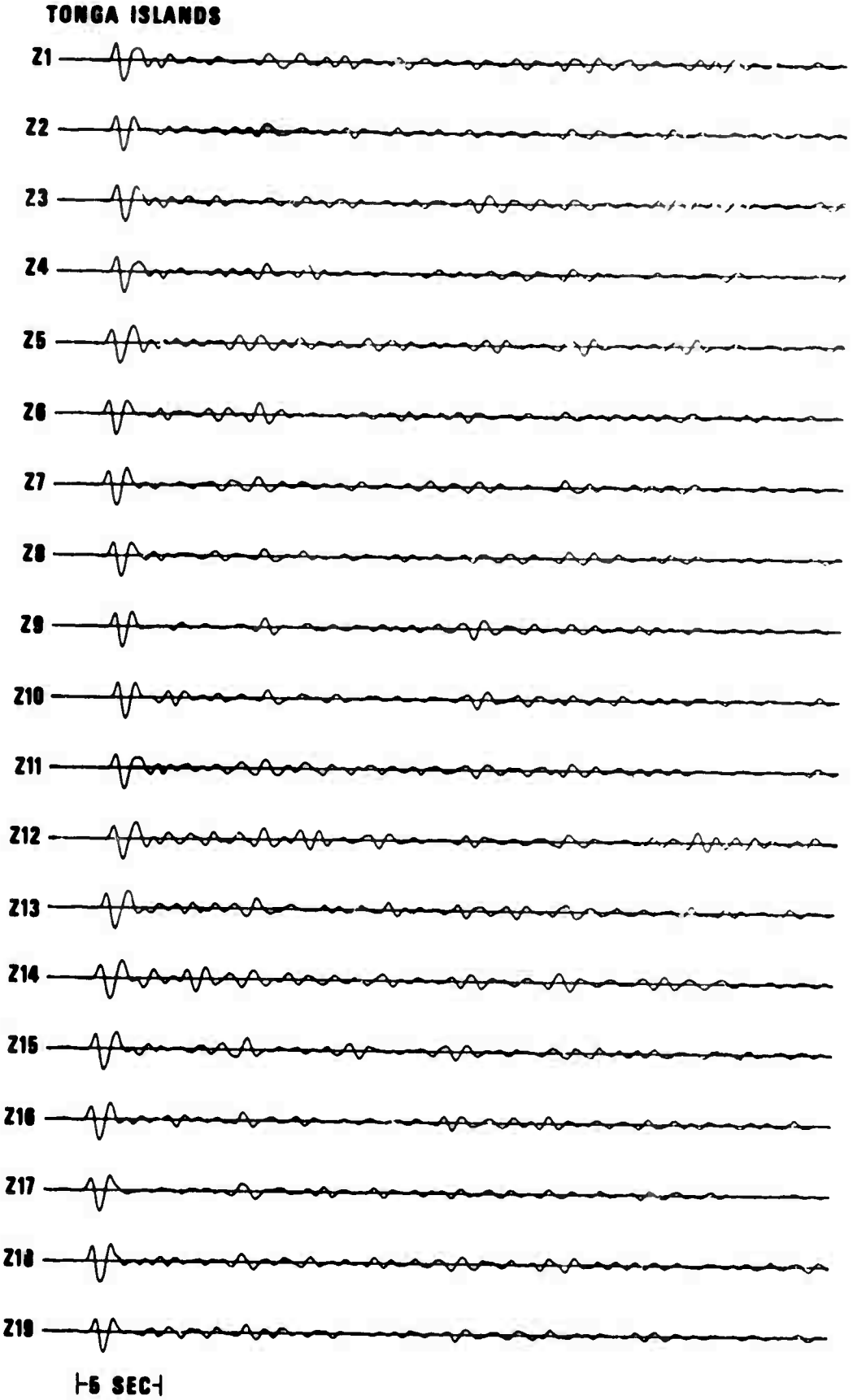

Figure 8. Seismograms for the Tonga Islands event.

$$\bar{R} = \frac{1}{N} \sum_{i=1}^{N} \left[\frac{1}{T} \sum_{t=1}^{T} s_i^2(t) \right]^{1/2}$$

where

$s_i(t)$ is the amplitude of the i^{th} channel at time t;

T is the length of the sample analyzed (the first 35 seconds of the signal in this work);

N is the number of channels processed (7 or 19 in this report).

If $\hat{s}_B(t)$ is the estimate for the leakage signal determined for the beam, then

$$\bar{R}_B = \left[\frac{1}{T} \sum_{t=1}^{T} \hat{s}_B^2(t) \right]^{1/2}$$

is a measure of the rms power in $\hat{s}_B(t)$. Similarly, a measure of the rms power in the mixed-signal estimate $\hat{s}_S(t)$ is:

$$\bar{R}_S = \left[\frac{1}{T} \sum_{t=1}^{T} \hat{s}_S^2(t) \right]^{1/2} .$$

The coda attenuation figures are then given by:

$$A_B = 20 \log \frac{\overline{R}_B}{\overline{R}}, \quad \text{and} \quad A_S = 20 \log \frac{\overline{R}_S}{\overline{R}}$$

The analysis is performed at a set of uniformly spaced azimuths, yielding polar plots of the coda attenuation capabilities for the beam and the mixed-signal processor. Note that this analysis method is equivalent to looking at the coda suppression obtainable on that portion of signal 1 which arrives ahead of signal 2.

As the events ranged from 38 to 85° distance from TFO, a nominal epicentral distance for the earthquake of 60° was chosen for this study. Further, computations are performed at an azimuthal interval of 30° (0°, 30°, 60°,...330°), with additional analyses performed every 10° in the vicinity of the test site azimuth. The test site used is Semipalatinsk (50°N, 78°E), at an epicentral distance of 95.9° from TFO and a station-to-test site azimuth of 354°. This test site is the epicenter for event 2, the (non-existant) signals of which we assume are masked by the signals from event 1.

RESULTS

Polar plots of coda attenuation are given in Figures 9 through 18. Results for the 7- and 19-element subarrays are paired by event. With but one minor exception (Fiji Islands, 19-element array, 180° azimuth), the coda attenuation capability of the mixed-signal processor exceeds that of the beam. While up to 14 db improvement over the beam is obtained (Easter Island, 19-element array, 30° azimuth), the improvement is generally on the order of 3 to 5 db for both subarrays. The maximum coda attenuation obtained using the mixed-signal processor and the 19-element subarray is 22 db (Fox Islands, 19-element array, 180° azimuth), with a nominal maximum value of 18 db being fairly representative. With respect to the 7-element subarray, the maximum attenuation obtained using the mixed-signal processor is about 17 db (Fox Islands, 120° azimuth), with 14 db being a more representative figure. In general the coda attenuation obtained using the 7-element subarray and the mixed-signal processor is comparable to that obtained using the 19-element array and the beam processor.

To determine the effect of narrowing the signal bandpass, data for the Fox and Tonga Islands events were filtered from 0.8 to 2 Hz (3 db points), and analyzed using the beam and mixed-signal processor. The results, shown in Figures 19 through 22, are essentially the same as those obtained previously using a filter bandpass of 0.4 to 3.0 Hz; thus, there appears

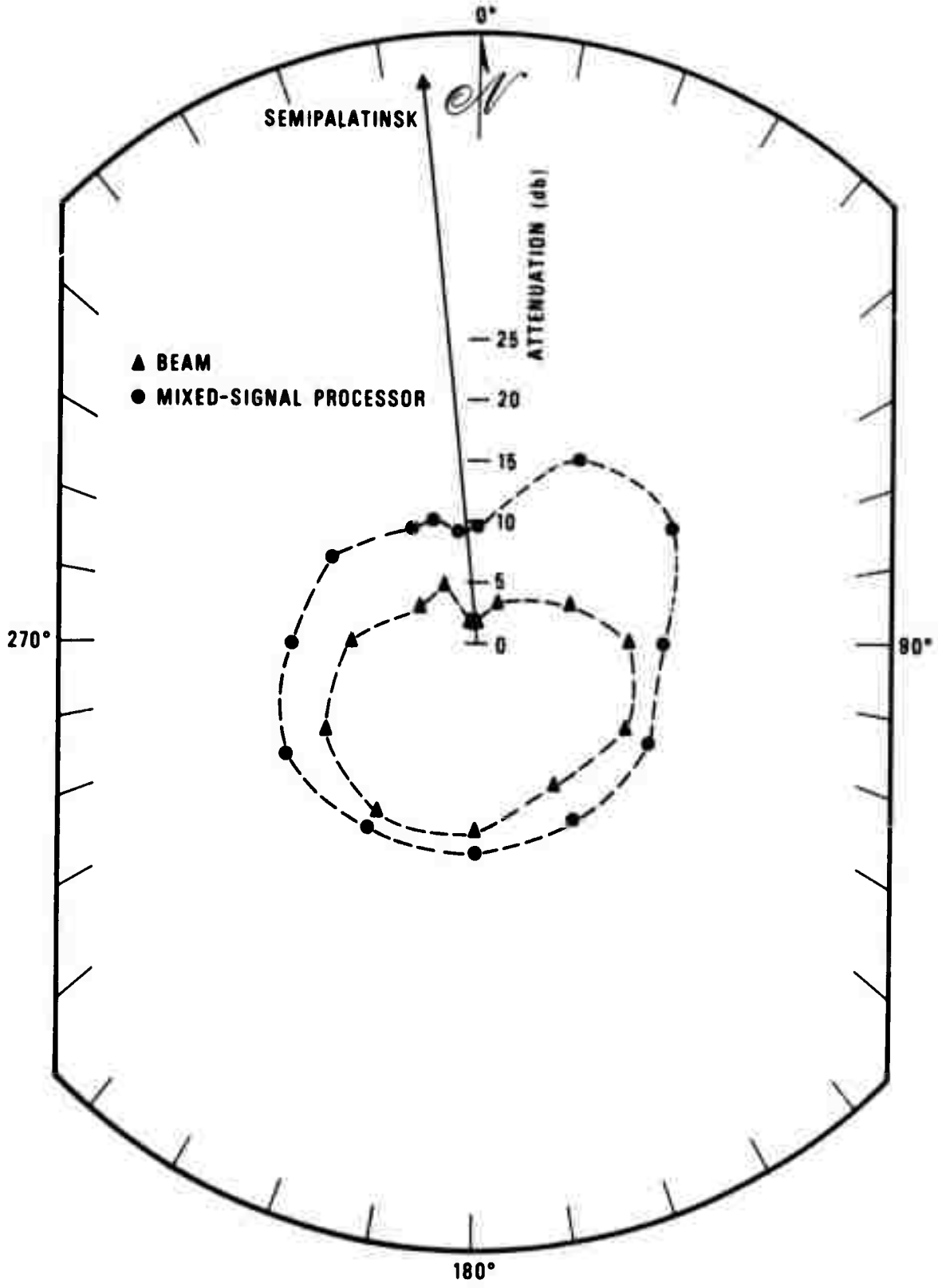

Figure 9. Coda attenuation, 19-element subarray, Easter Island event, seismograms bandpass filtered with 3 db points at 0.4 and 3.0 Hz.

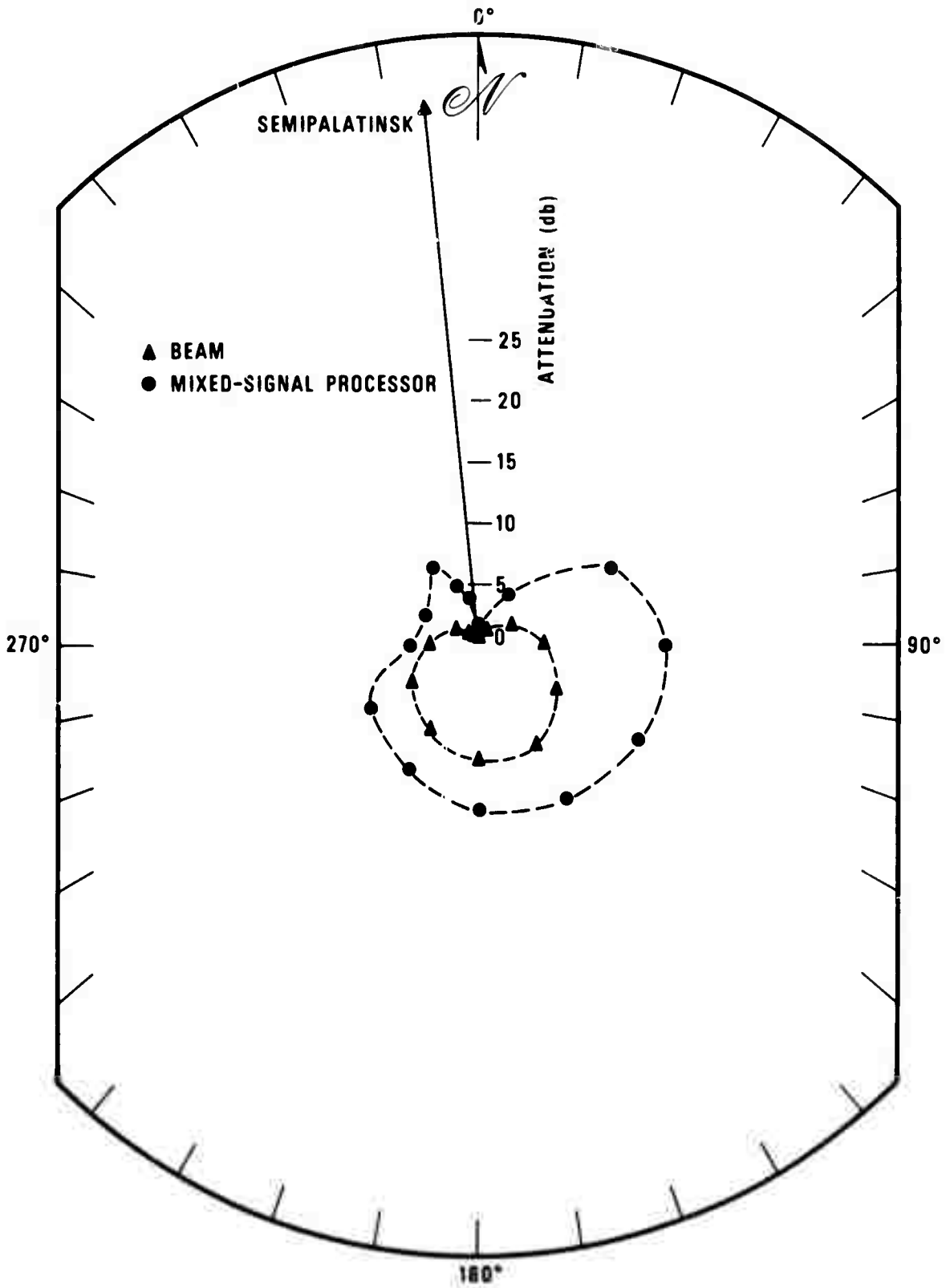

Figure 10. Coda attenuation, 7-element subarray, Easter Island event, seismograms bandpass filtered with 3 db points at 0.4 and 3.0 Hz.

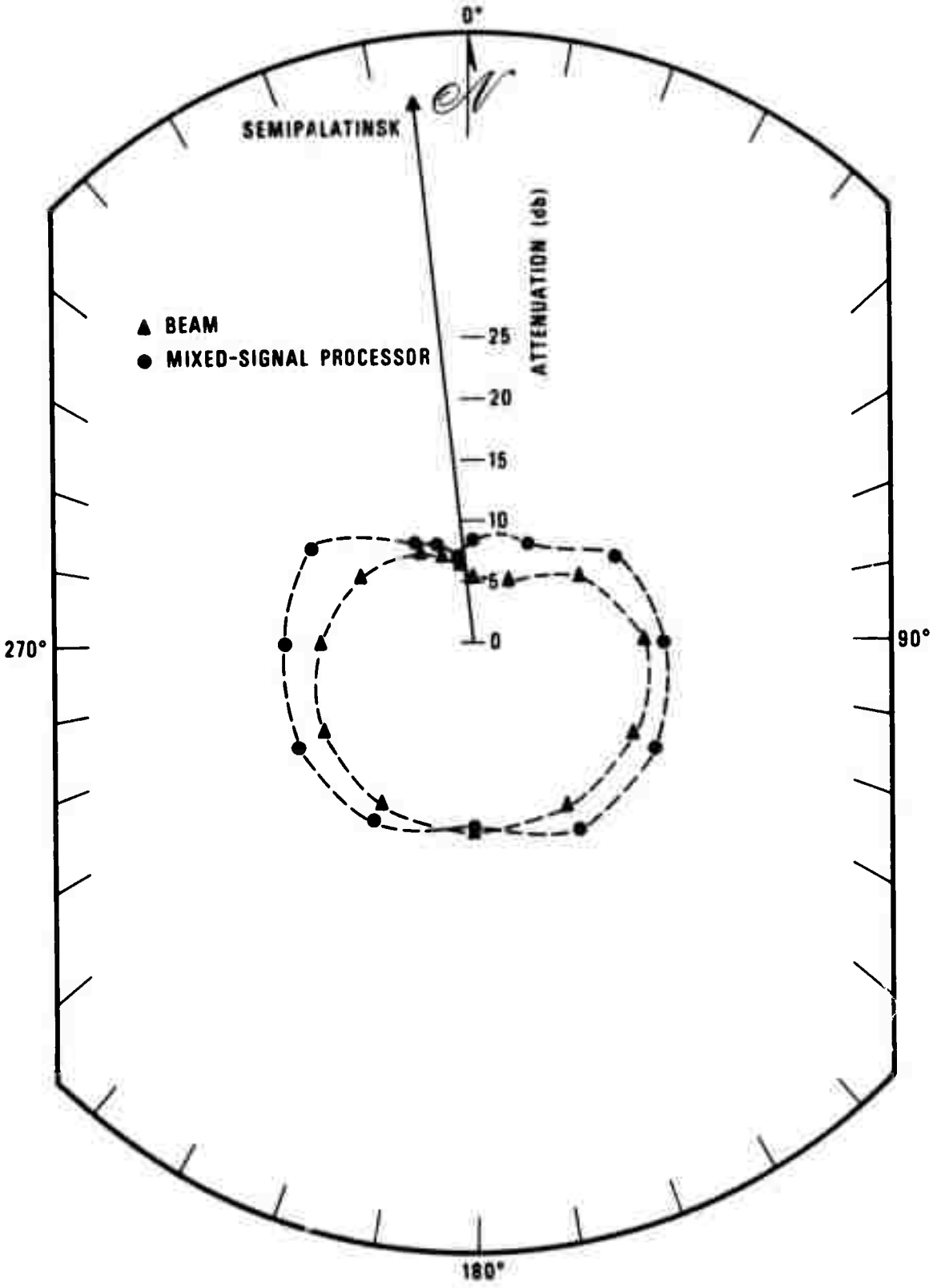

Figure 11. Coda attenuation, 19-element subarray, Fiji Islands event, seismograms bandpass filtered with 3 db points at 0.4 and 3.0 Hz.

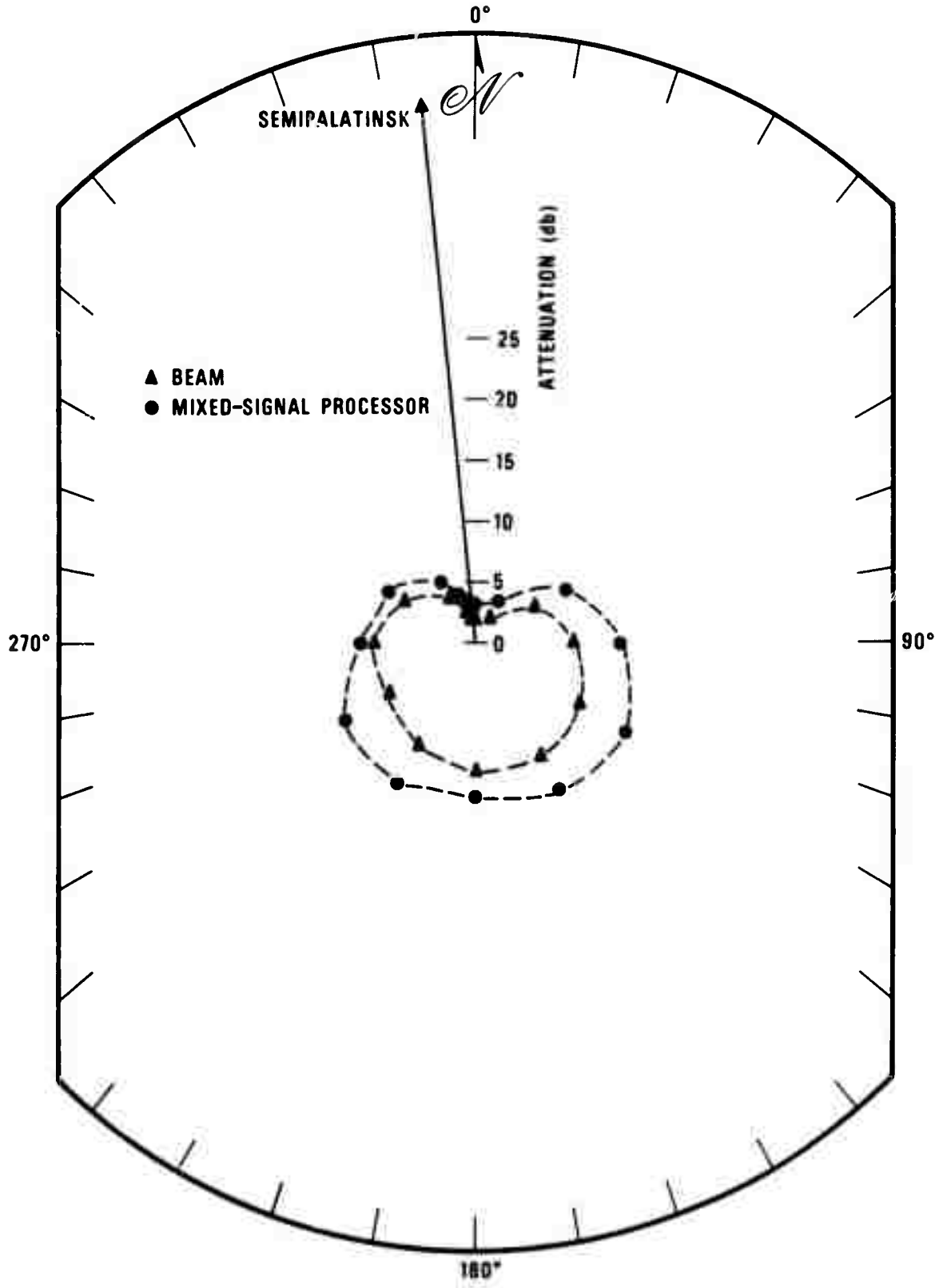

Figure 12. Coda attenuation, 7-element subarray, Fiji Islands event, seismograms bandpass filtered with 3 db points at 0.4 and 3.0 Hz.

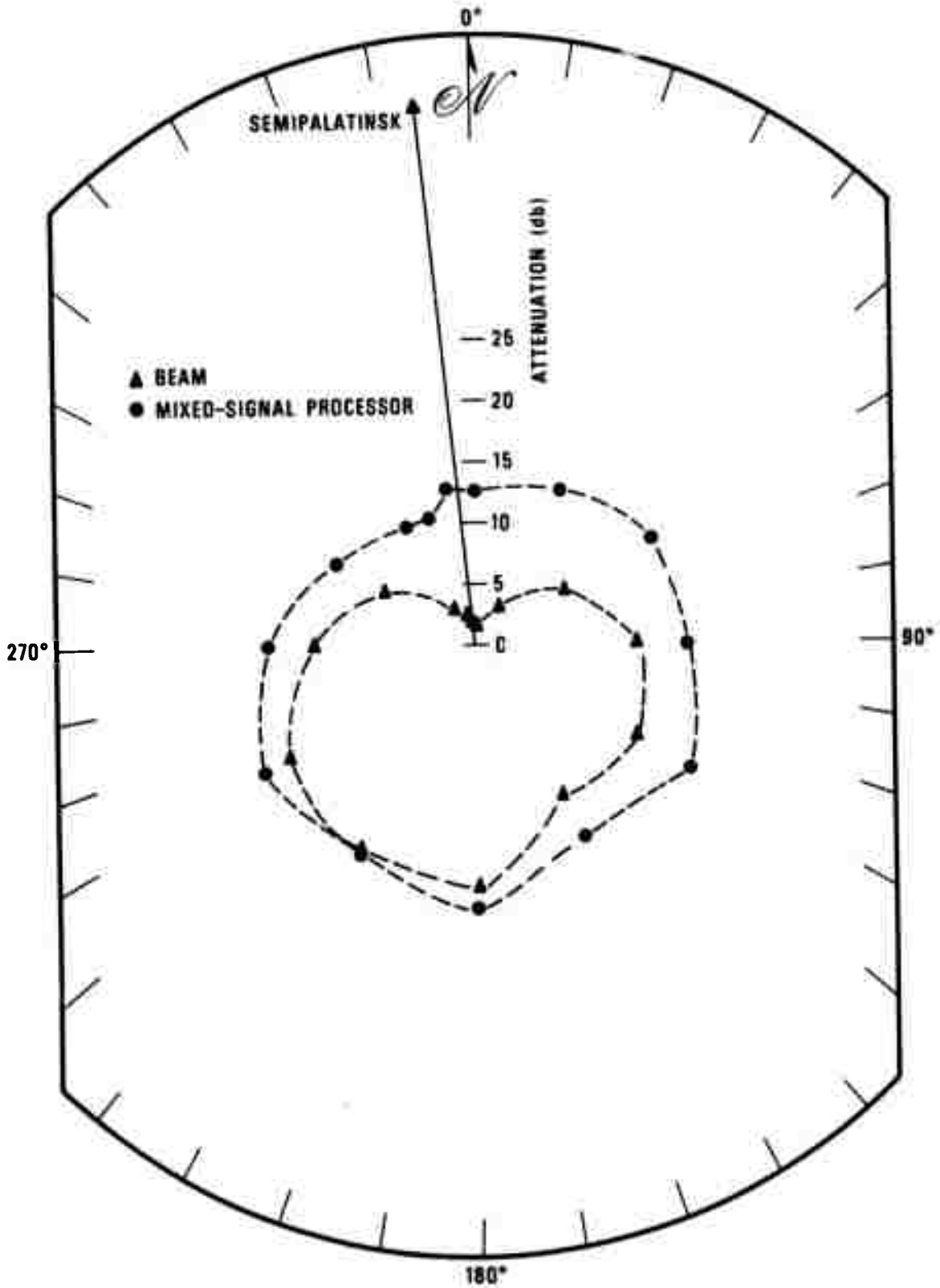

Figure 13. Coda attenuation, 19-element subarray, Fox Islands event, seismograms bandpass filtered with 3 db points at 0.4 and 3.0 Hz.

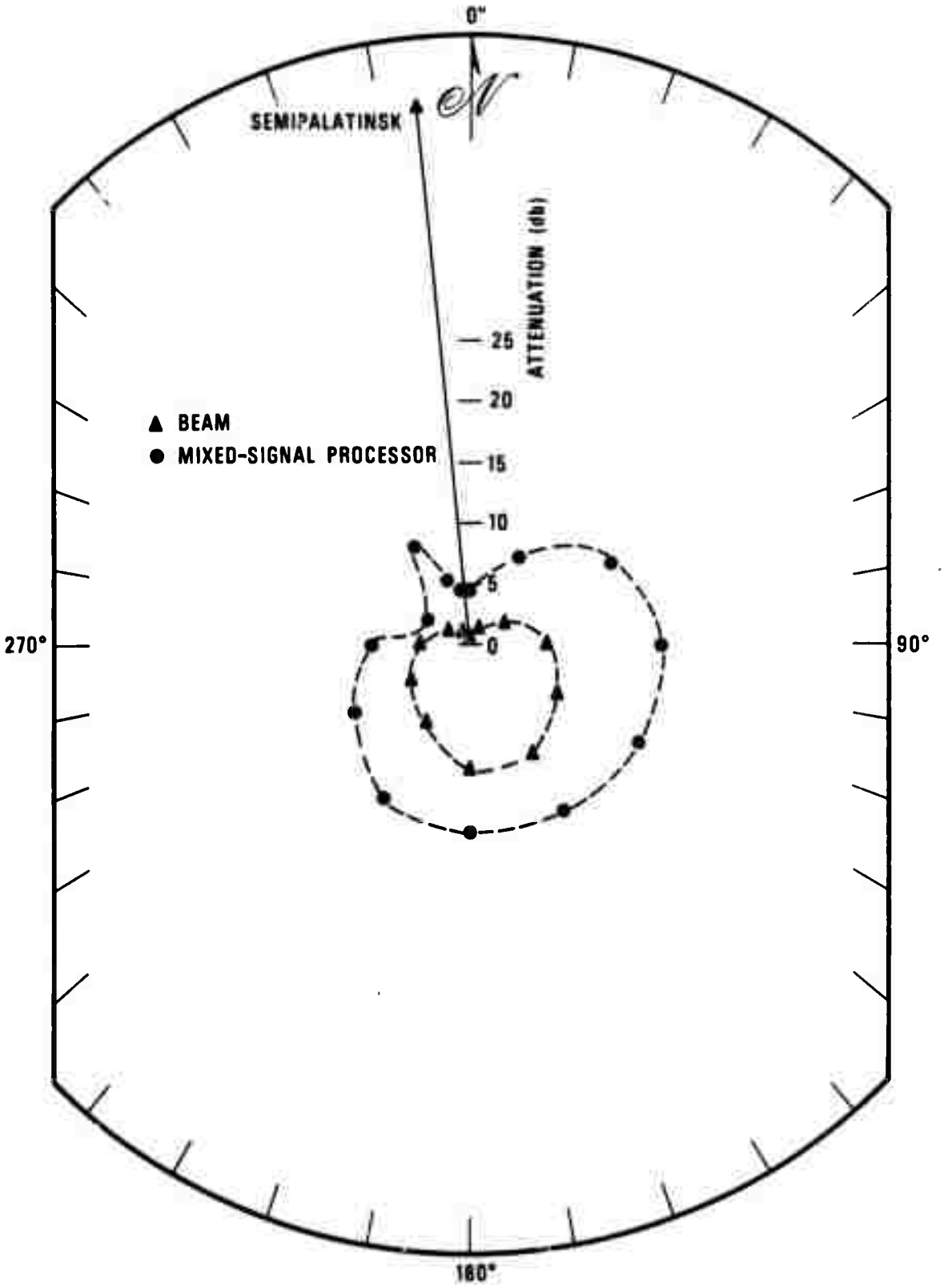

Figure 14. Coda attenuation, 7-element subarray, Fox Islands event, seismograms bandpass filtered with 3 db points at 0.4 and 3.0 Hz.

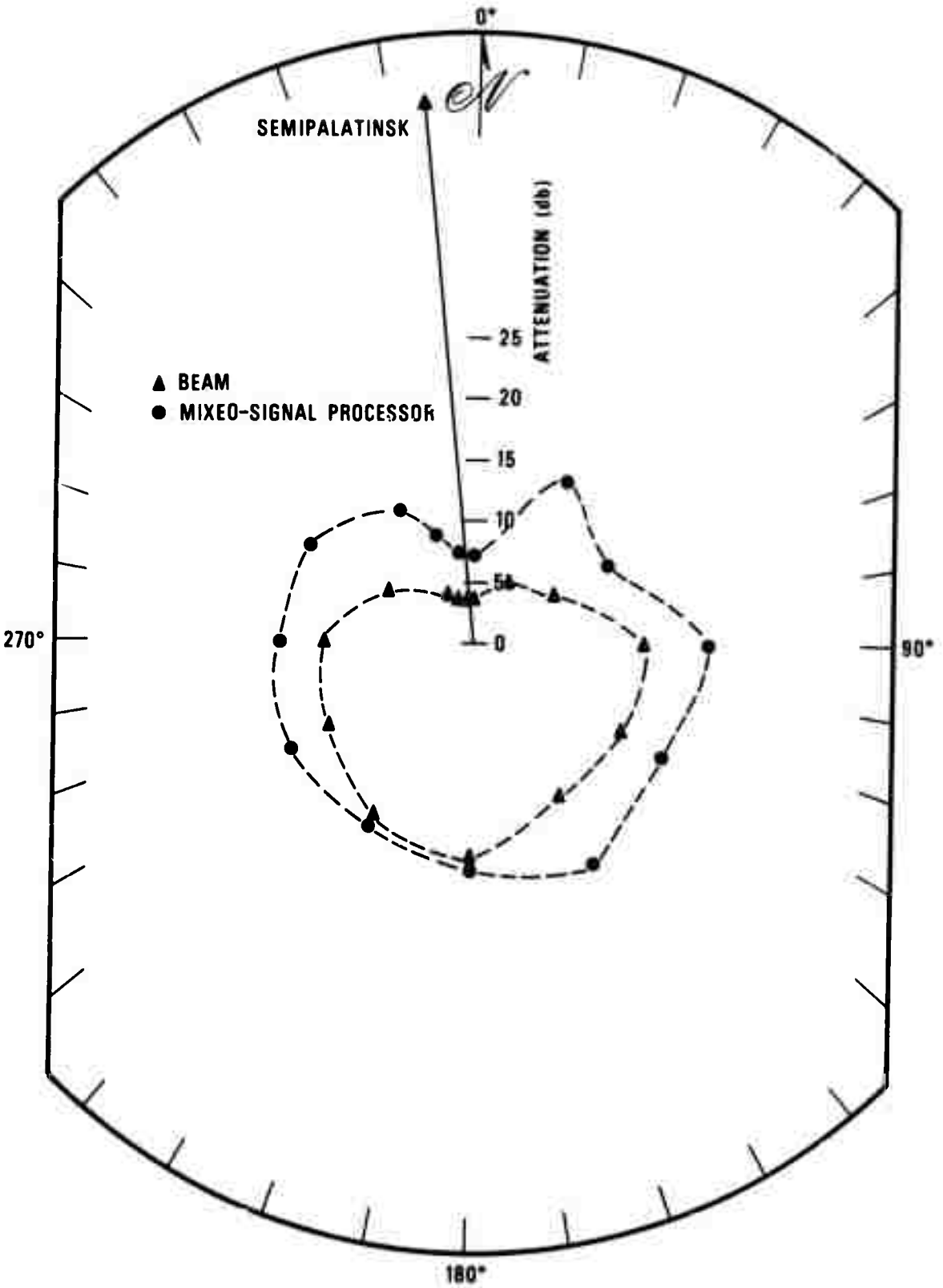

Figure 15. Coda attenuation, 19-element subarray, Hokkaido event, seismograms bandpass filtered with 3 db points at 0.4 and 3.0 Hz.

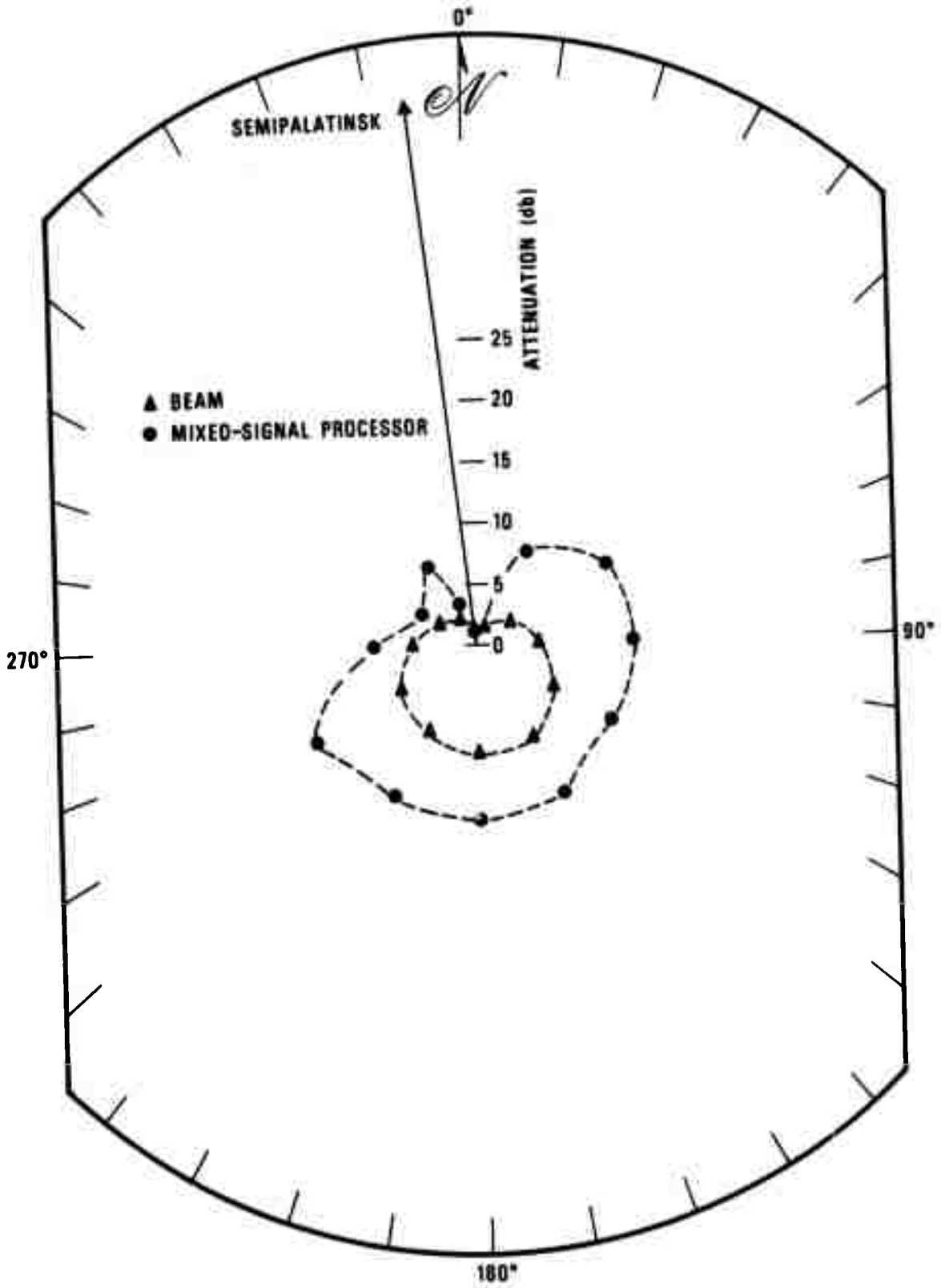

Figure 16. Coda attenuation, 7-element subarray, Hokkaido event, seismograms bandpass filtered with 3 db points at 0.4 and 3.0 Hz.

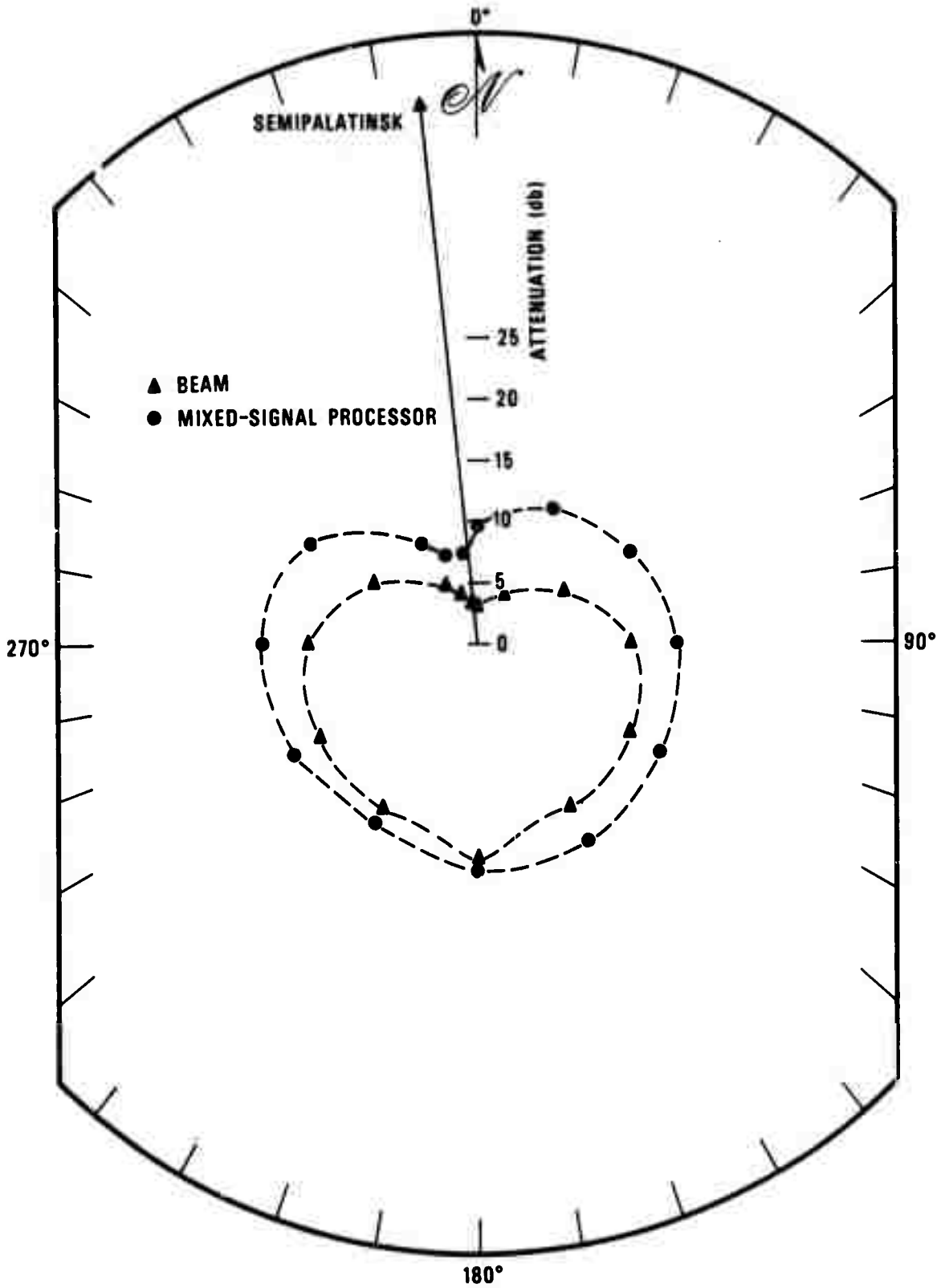

Figure 17. Coda attenuation, 19-element subarray, Tonga Island event, seismograms bandpass filtered with 3 db points at 0.4 and 3.0 Hz.

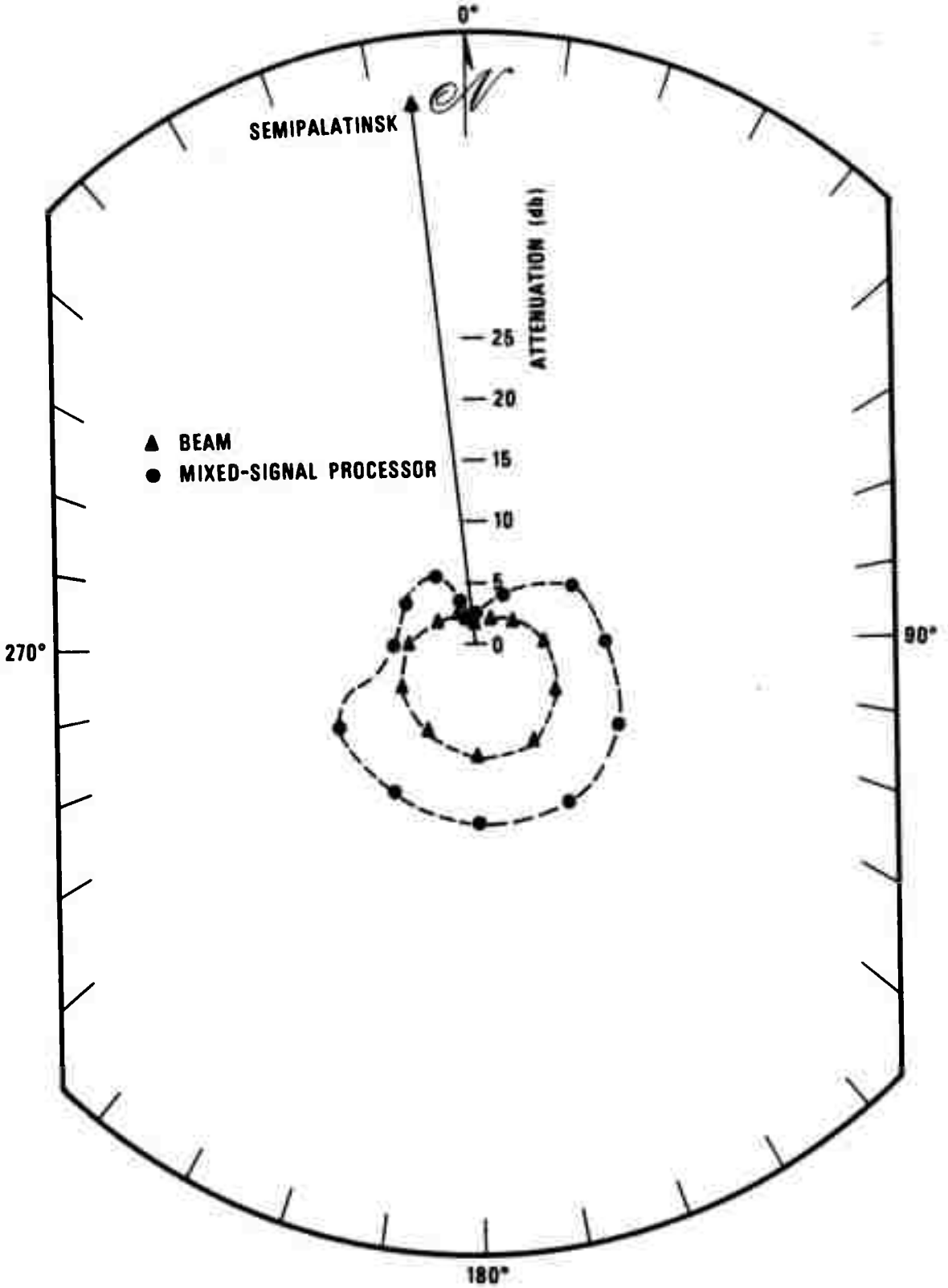

Figure 18. Coda attenuation, 7-element subarray, Tonga Island event, seismograms bandpass filtered with 3 db points at 0.4 and 3.0 Hz.

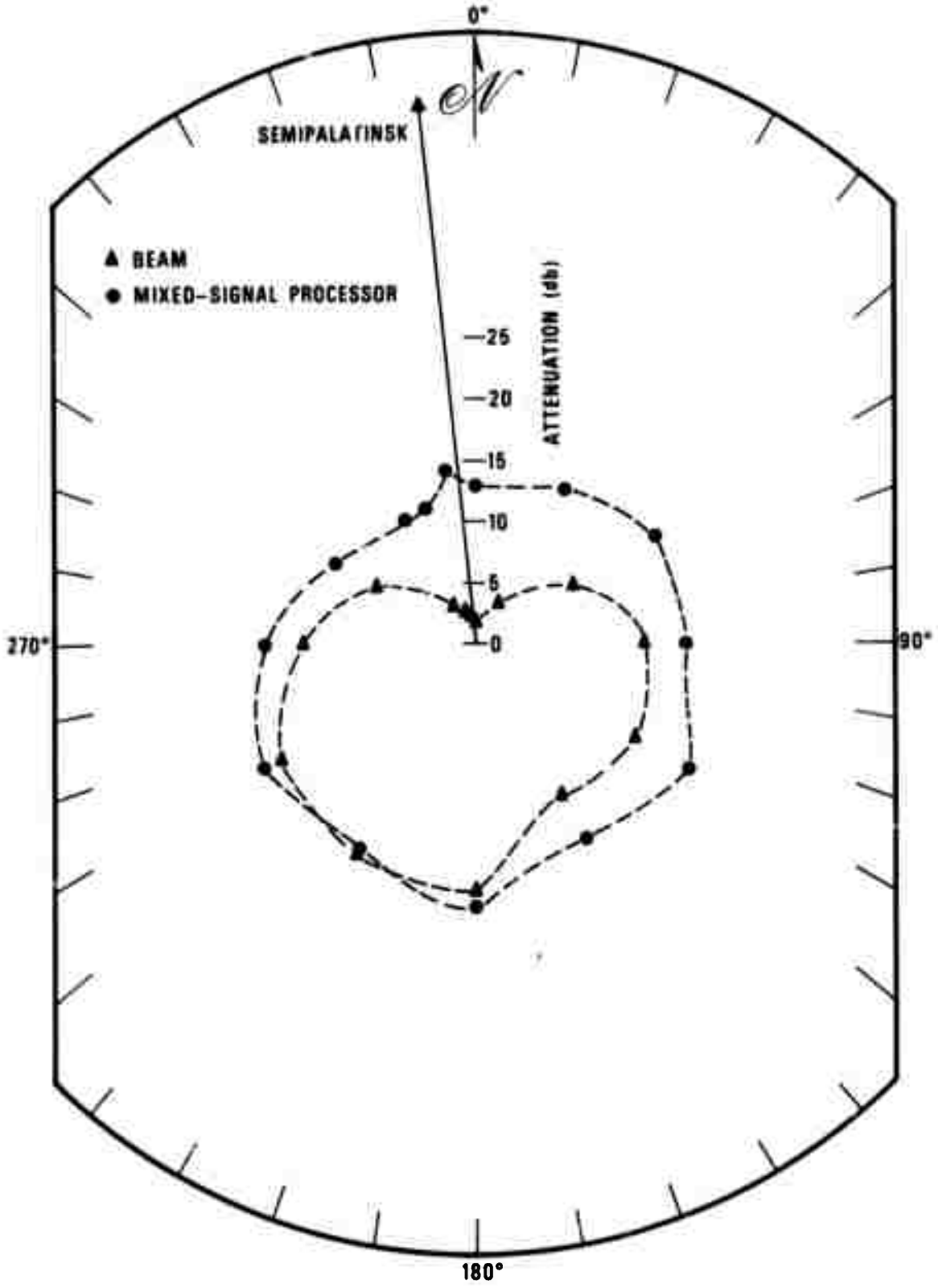

Figure 19. Coda attenuation, 19-element subarray, Fox Islands event, seismograms bandpass filtered with 3 db points at 0.4 and 3.0 Hz.

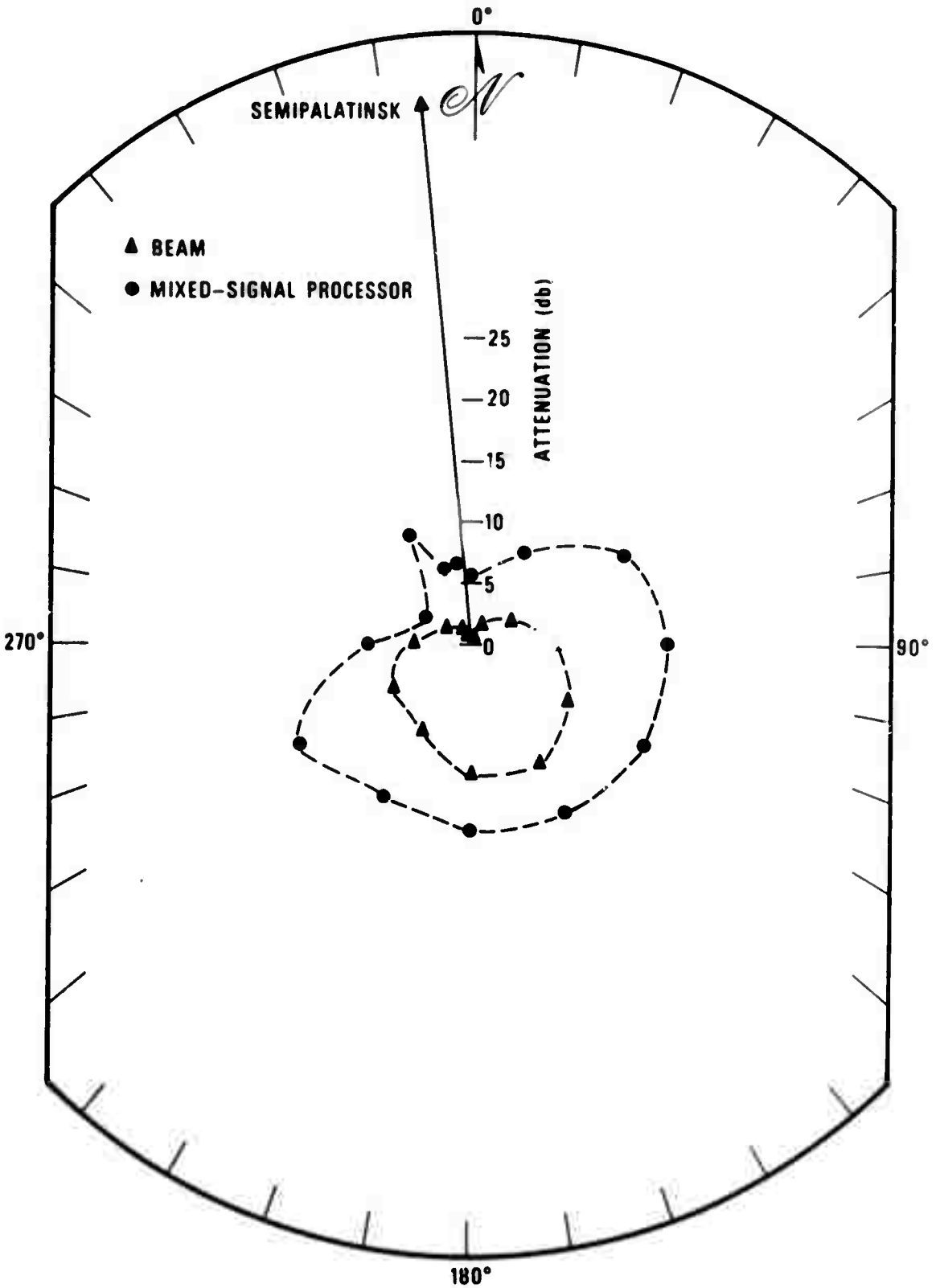

Figure 20. Coda attenuation, 7-element subarray, Fox Islands event, seismograms bandpass filtered with 3 db points at 0.4 and 3.0 Hz.

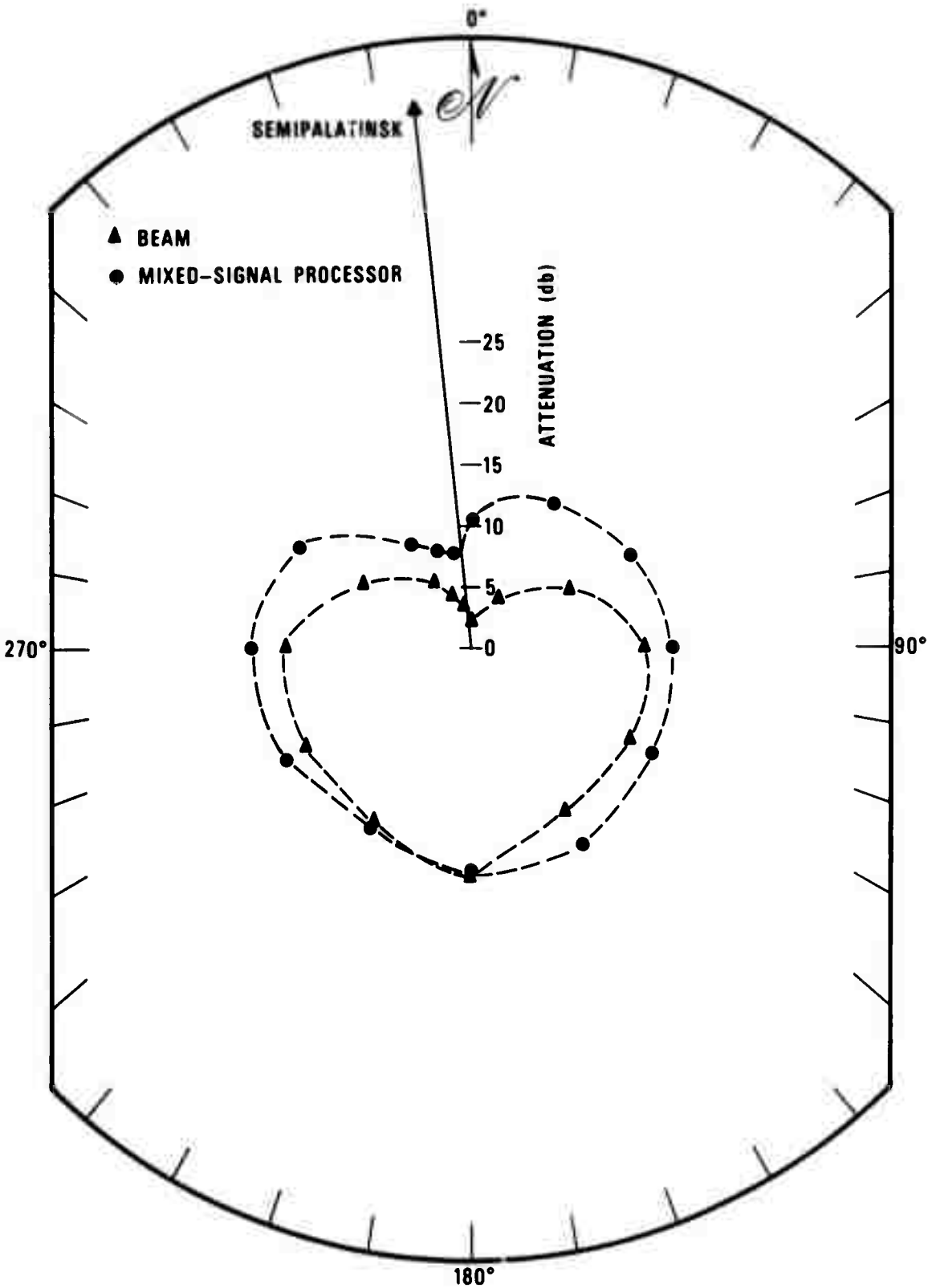

Figure 21. Coda attenuation, 19-element subarray, Tonga Islands event, seismograms bandpass filtered with 3db points at 0.8 and 2.0Hz.

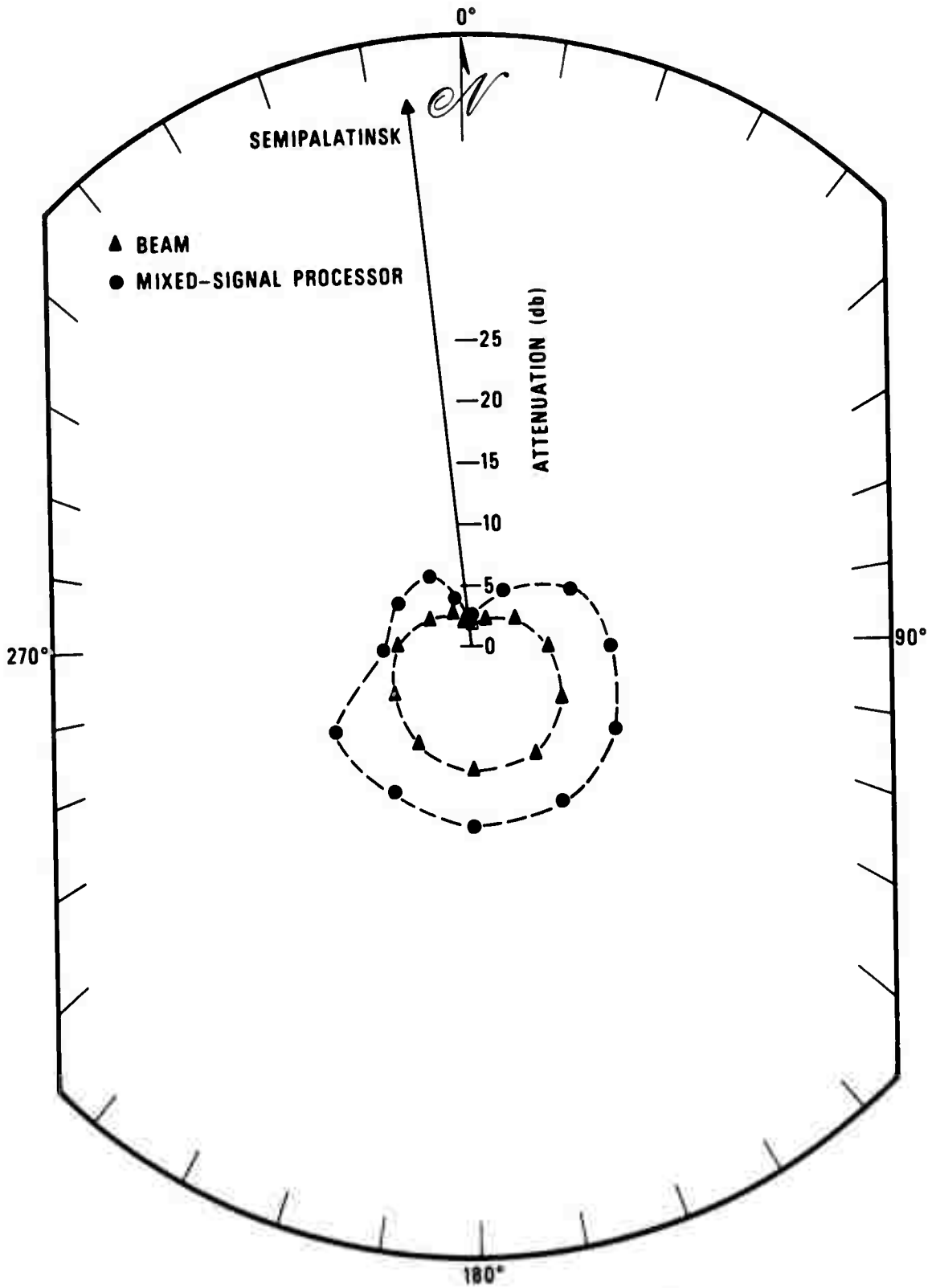

Figure 22. Coda attenuation, 7-element subarray, Tonga Islands event, seismograms bandpass filtered with 3db points at 0.8 and 2.0Hz.

to be no advantage in using narrow-bandpassed data for coda attenuation.

The general shape of the coda attenuation curves suggests that these data can be represented analytically by the following formula:

$$\rho = a - b \cdot \cos(\theta+\alpha) \text{ db} \tag{4}$$

where α is a fixed rotation angle to orient the attenuation pattern. In the cases examined in this work, $\alpha = 6°$. Least square fits to the data sets shown in Figures 9 through 18 yield the estimates for a and b shown in Table III. The average coda attenuation characteristics are shown in Figures 23 and 24. Here, the coda attenuation curves have been rotated by 6°, implying that the event to be masked is arriving from the north.

While it is convenient to describe the attenuation data in the functional form [a - b·cos(θ+α) db], these curves are only partially useful in describing the capabilities of a given array and processor. We would like to have more general analytical expressions for coda suppression. Such curves can be derived by plotting the attenuation data as a function of the difference in the ray parameters for the two signals:

$$\delta\left(\frac{dT}{d\Delta}\right) \equiv \left|\left(\frac{\vec{dT}}{d\Delta}\right)_1 - \left(\frac{\vec{dT}}{d\Delta}\right)_2\right|$$

TABLE III

Coda Attenuation Parameters

Source Region: Semipalatinsk

$\rho = a - b \cdot \cos(\theta + 6°)$

REGION	19-ELEMENT SUBARRAY				7-ELEMENT SUBARRAY			
	BEAM		MIXED-SIGNAL PROCESSOR		BEAM		MIXED-SIGNAL PROCESSOR	
	a (db)	b (db)	a (db)	b (db)	a (db)	b (db)	a (db)	b (db)
Easter Island	9.9	7.0	15.3	3.1	4.8	4.3	9.8	4.5
Fiji Islands	12.0	4.9	14.0	4.5	7.2	4.2	9.8	5.0
Fox Islands	11.5	8.6	16.9	4.2	5.2	4.6	11.5	5.0
Hokkaido	11.0	6.7	15.5	4.7	5.2	3.8	10.2	5.3
Tonga Islands	11.2	6.9	15.1	4.7	5.5	3.7	9.7	5.9
AVERAGE	11.1	6.8	15.3	4.2	5.6	4.1	10.2	5.1

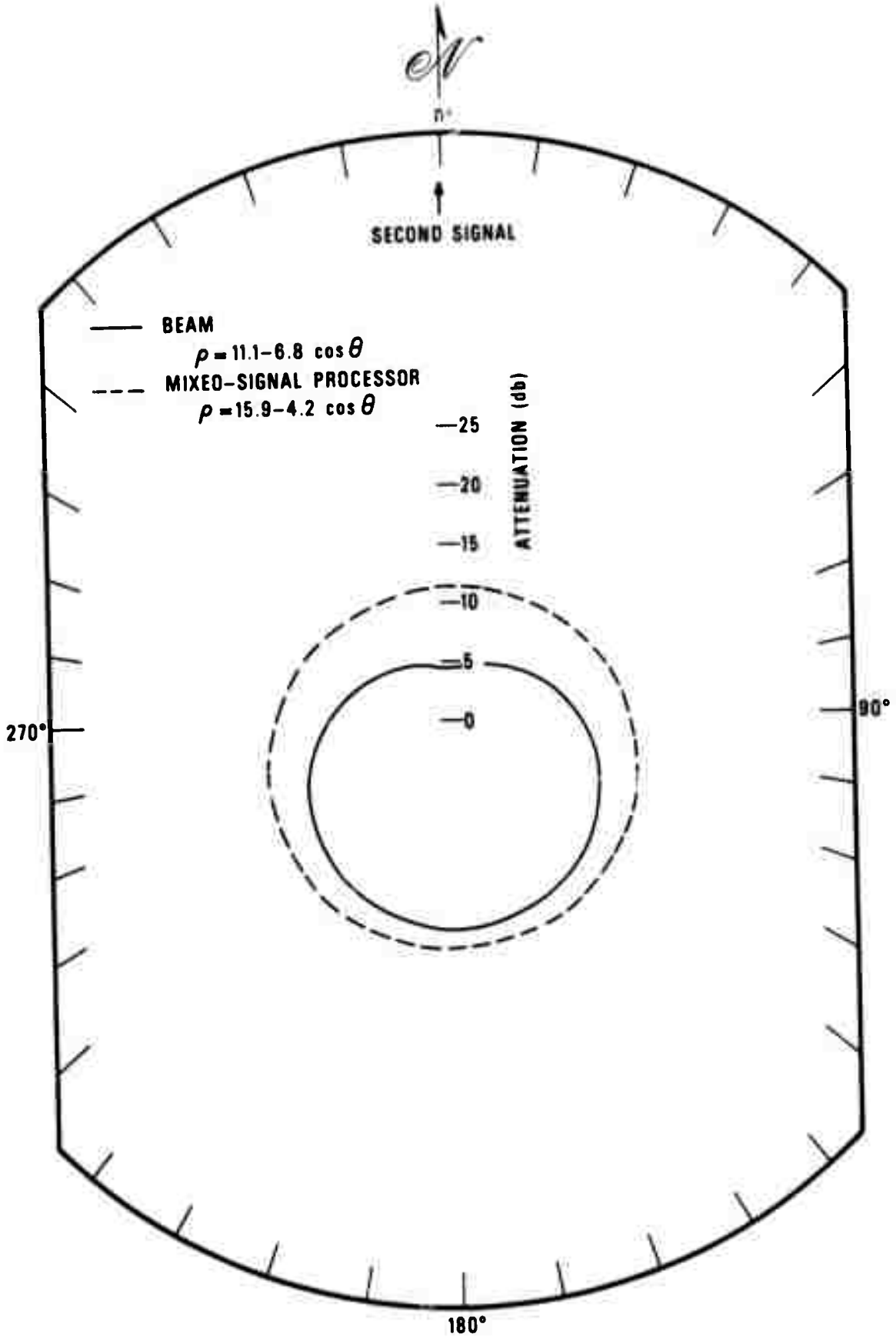

Figure 23. Average coda attenuation, 19-element subarray.

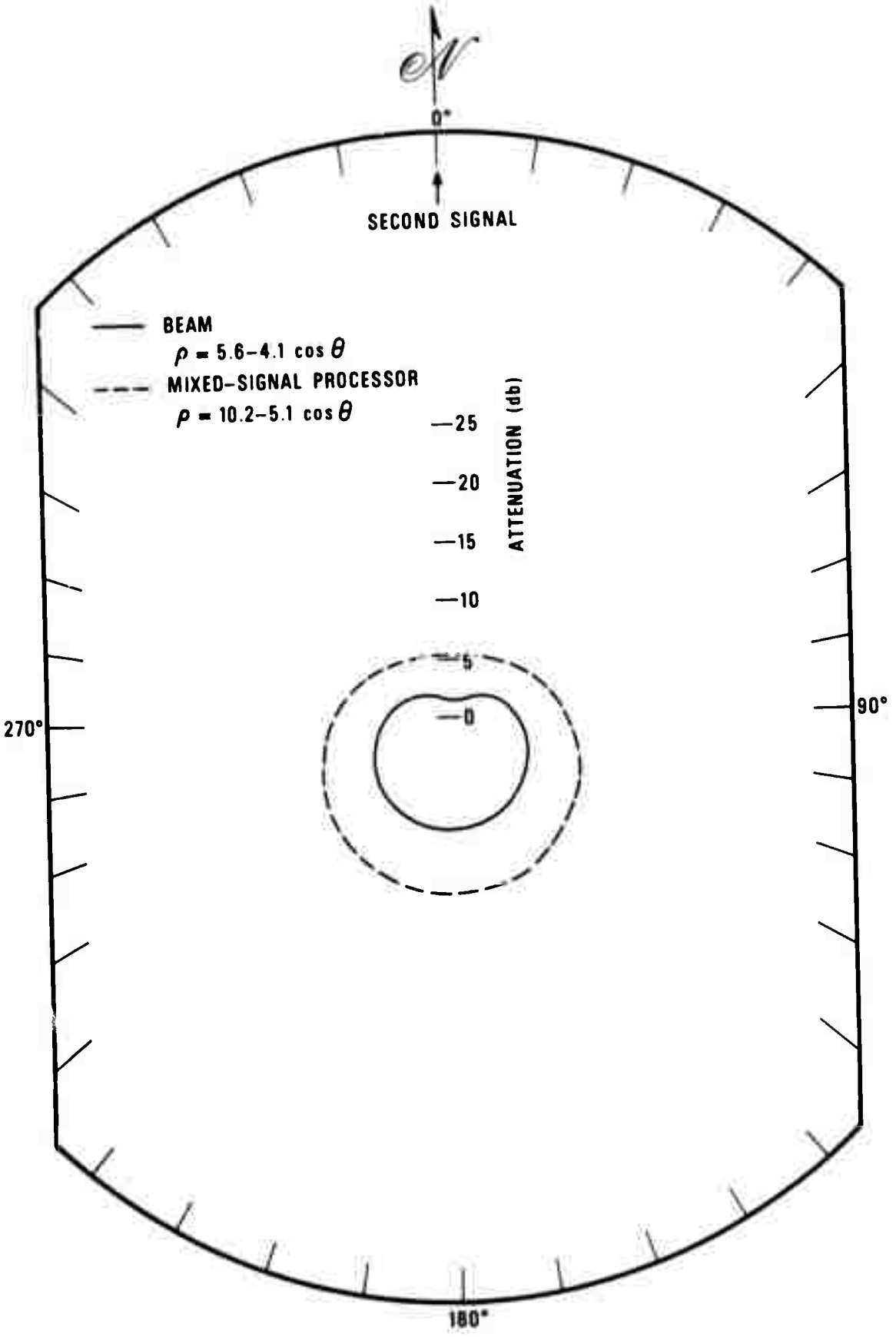

Figure 24. Average coda attenuation, 7-element subarray.

Figures 25 through 28 display the coda attenuation data as a function of $\delta(dt/d\Delta)$. Included here are the results obtained when the source region is taken as the Tonga Islands (Δ = 78°) and the masking event (Fox Islands event) is again taken at 60° distance (Figures 29 and 30; Table IV). The latter data set is included to help define trends in the attenuation characteristics, and is not used in subsequent numerical analyses.

We are guided in our choice of an analytical expression for the more generalized attenuation curves by the following observations:

I. Knowing that the generalized curves must pass through (0, 0) (no coda attenuation possible when both events have the same epicenter), the data suggest that for $\delta(dt/d\Delta)$ small, the coda attenuation curves are linear.

II. For $\delta(dT/d\Delta)$ large, the data appear to level off as if to approach asymptotically some limiting value.

Note that neither of these conditions is satisfied by the $[a - b \cdot \cos(\theta+\alpha)]$ model, which can only describe a portion of the more generalized curve.

One expression which can be used to describe the attenuation characteristics we observe is:

$$\rho = \frac{\beta X + \gamma X^2}{1.0 + \delta X + \varepsilon X^2} \text{ db}, \tag{5}$$

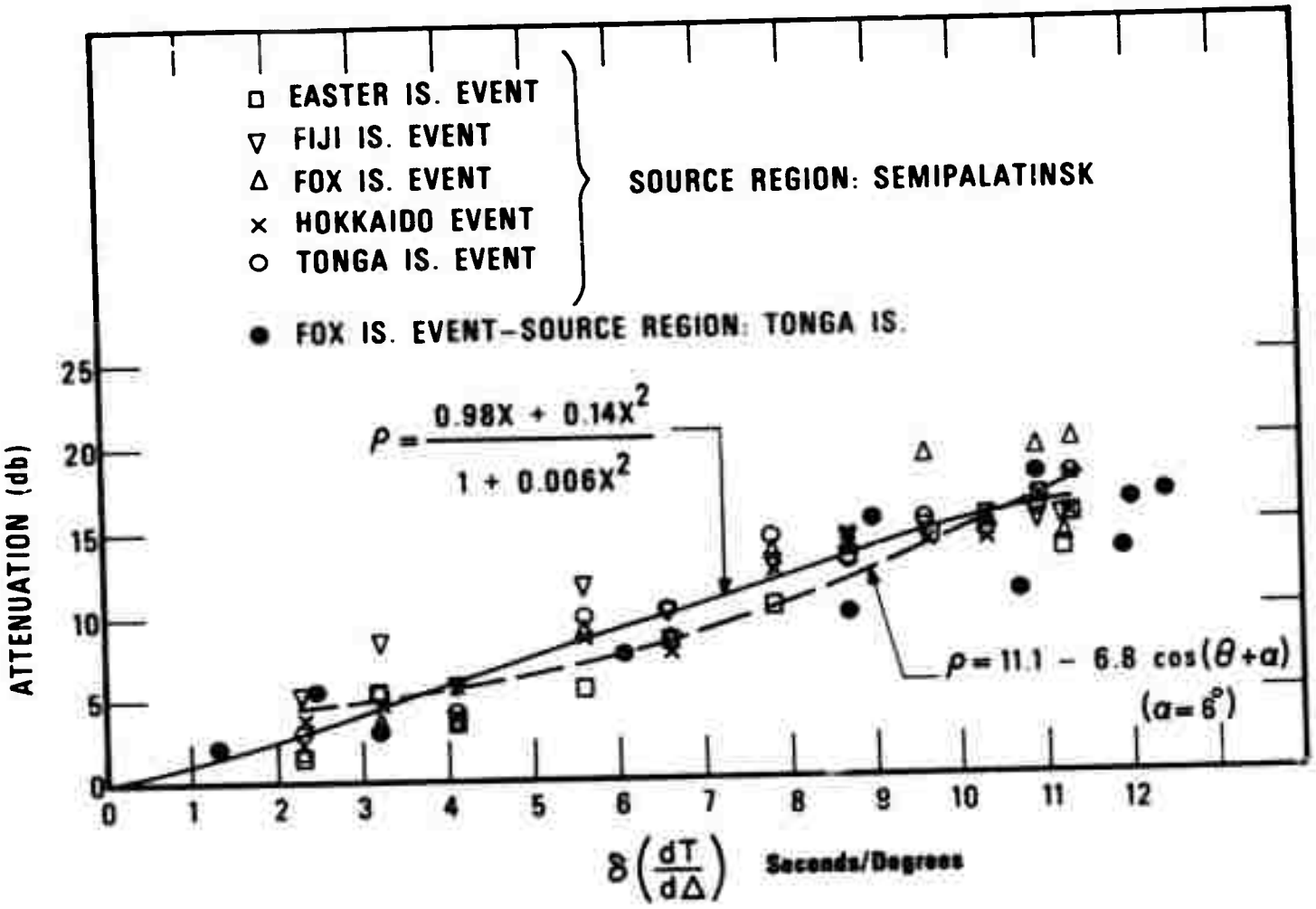

Figure 25. Attenuation as a function of the difference in ray parameters, 19-element subarray, beam.

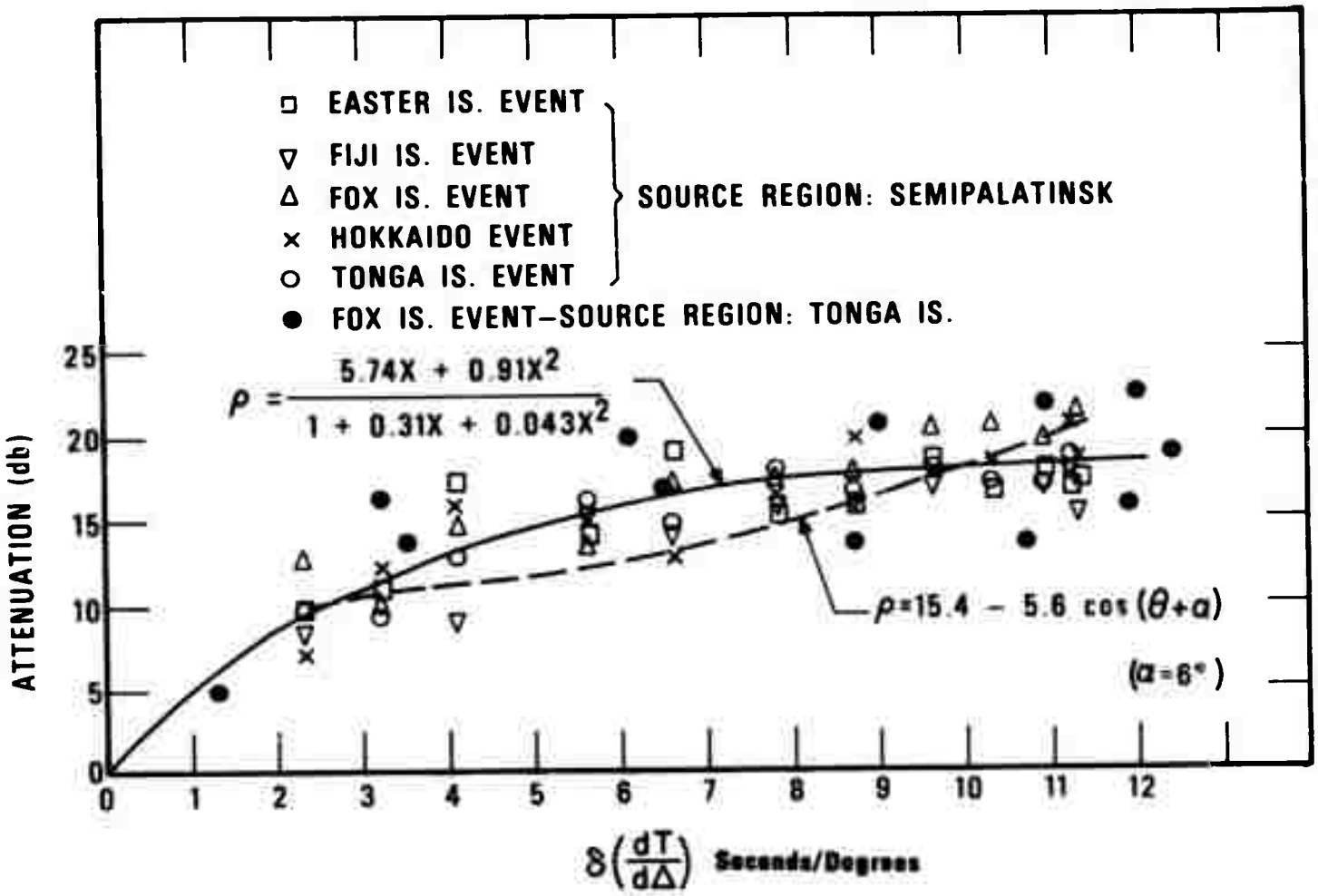

Figure 26. Attenuation as a function of the difference in ray parameters, 19-element subarray, mixed-signal processor.

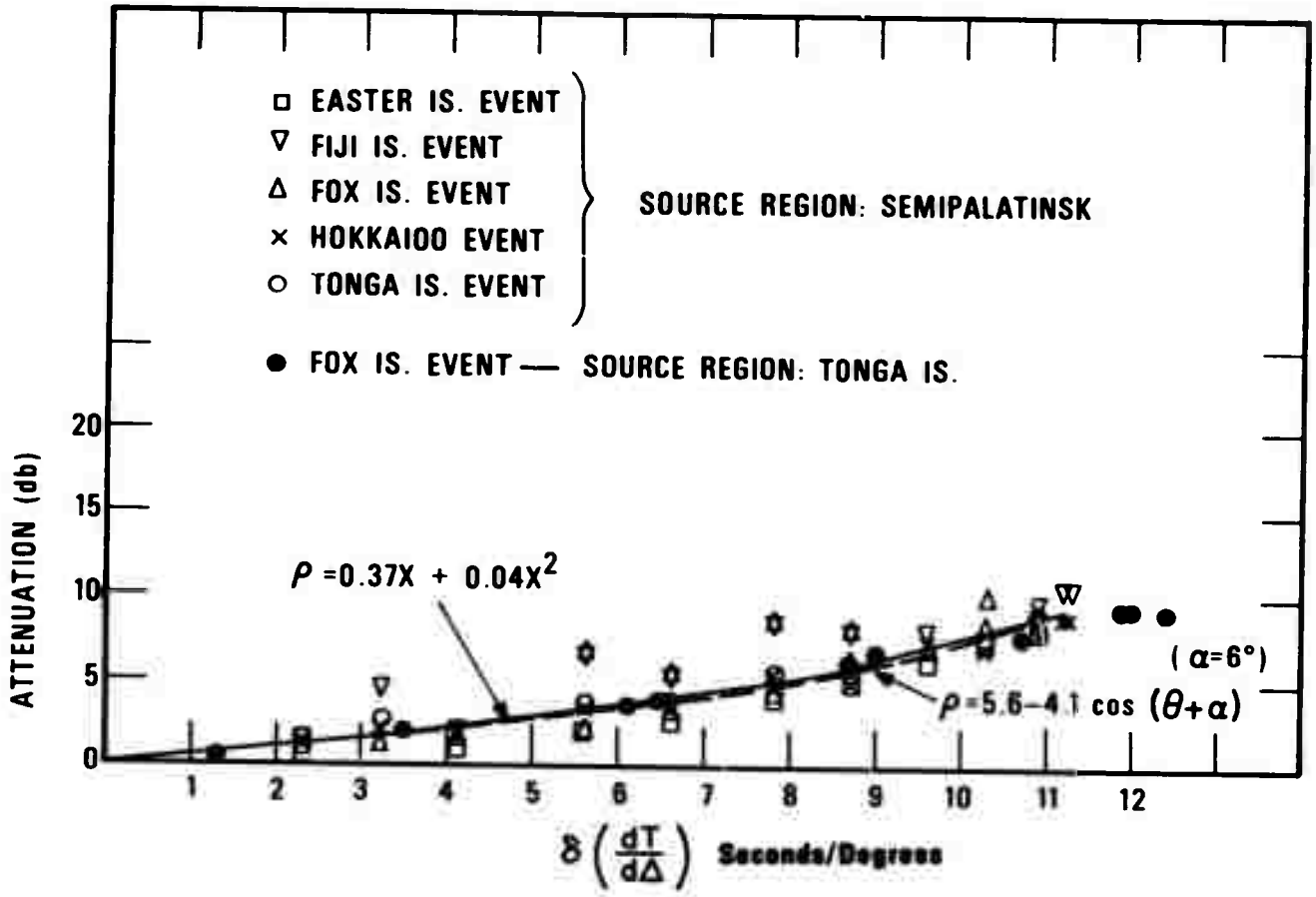

Figure 27. Attenuation as a function of the difference in ray parameters, 7-element subarray, beam.

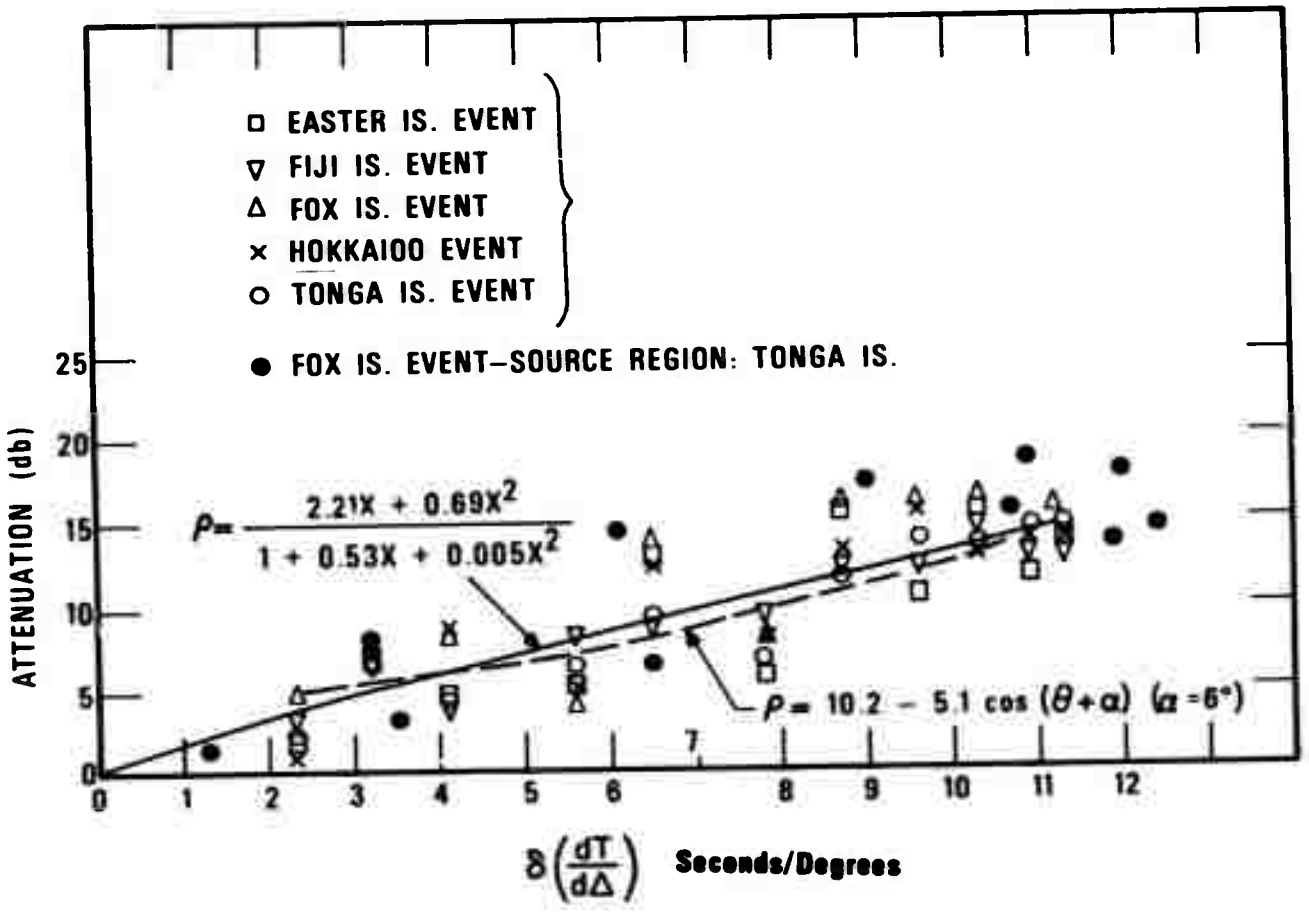

Figure 28. Attenuation as a function of the difference in ray parameters. 7-element subarray, mixed-signal processor.

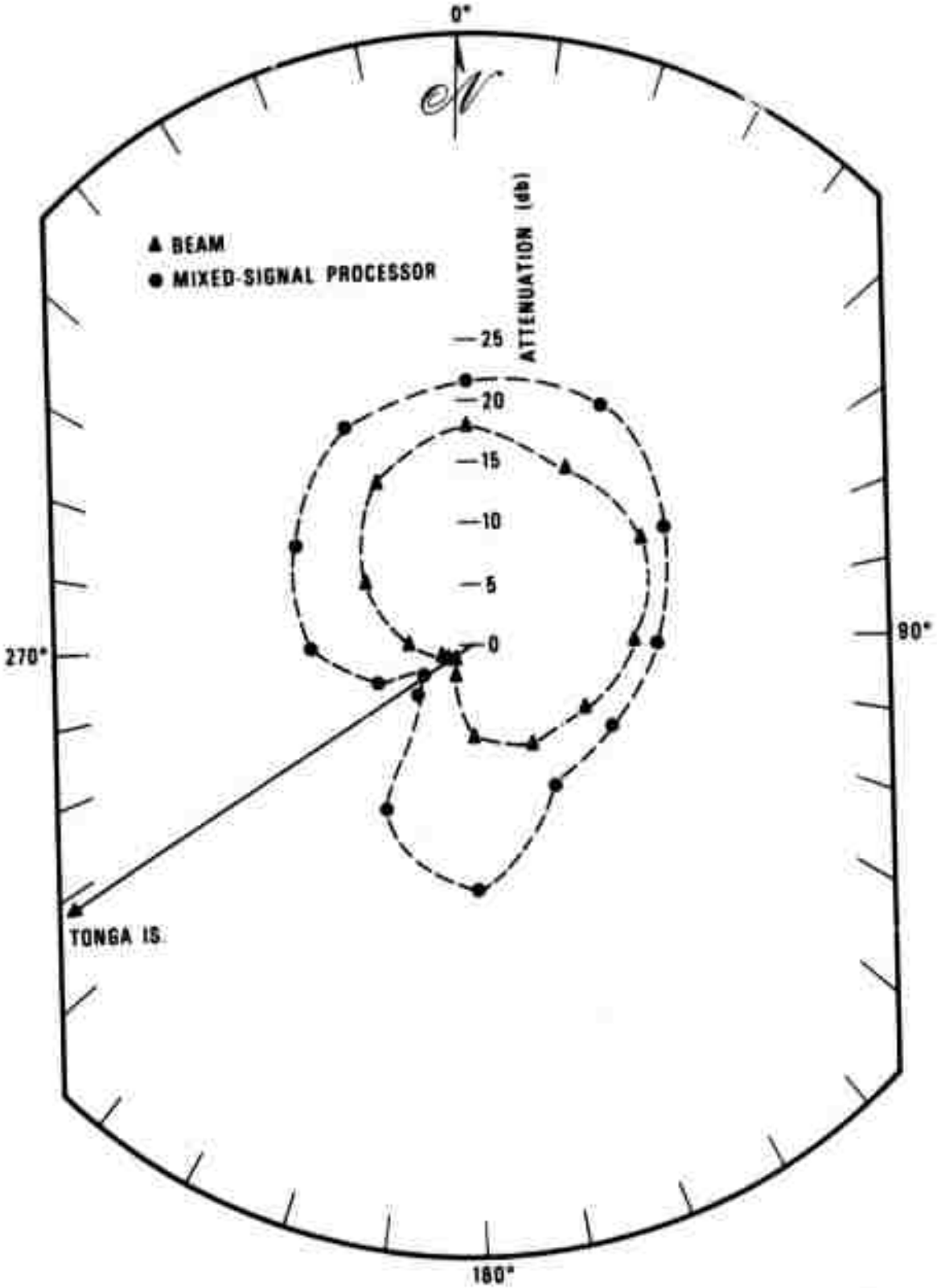

Figure 29. Coda attenuation, 19-element subarray, Fox Islands event, seismograms bandpass filtered with 3 db points at 0.4 and 3.0 Hz. (Signal 2 from Tonga Islands).

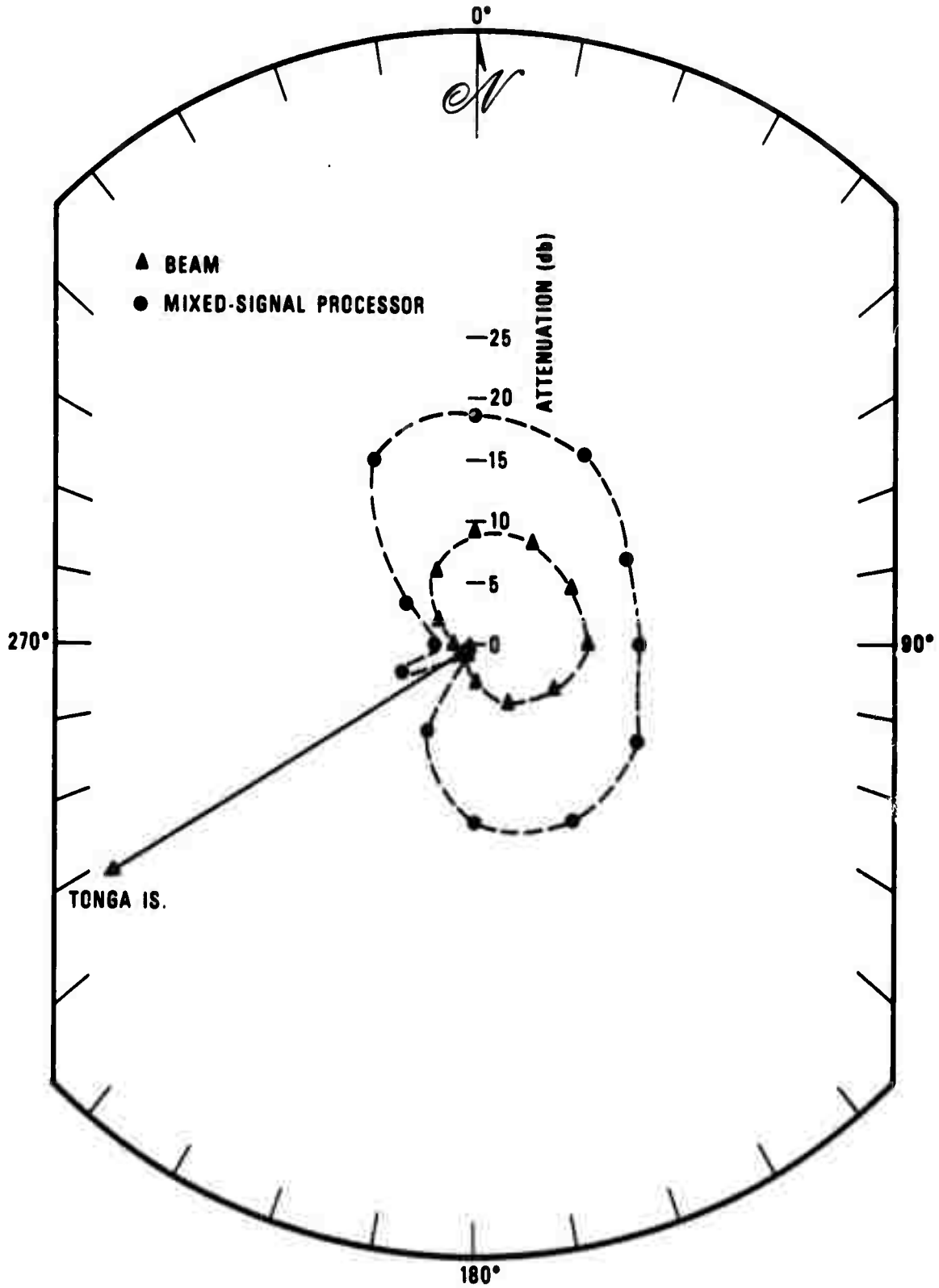

Figure 30. Coda attenuation, 7-element subarray, Fox Islands event, seismograms bandpass filtered with 3 db points at 0.4 and 3.0 Hz. (Signal 2 from Tonga Islands).

TABLE IV

Coda Attenuation Parameters

Source Region: Tonga Islands

$\rho = a - b \cdot \cos(\theta + 122°)$

	19-ELEMENT SUBARRAY				7-ELEMENT SUBARRAY			
	BEAM		MIXED-SIGNAL PROCESSOR		BEAM		MIXED-SIGNAL PROCESSOR	
REGION	a (db)	b (db)	a (db)	b (db)	a (db)	b (db)	a (db)	b (db)
Fox Islands	10.1	6.8	15.5	4.9	5.2	3.5	11.6	3.9

where

$$X \equiv \delta(dt/d\Delta)$$

Using equation (5) we obtain the least square solutions shown in Table V. These solutions are shown graphically in Figures 25 through 28. While some of the analytical expressions do not behave well at very large values of X, all of the solutions are acceptable in the region of interest. Note that for either array, the value for β determined from the mixed-signal data is almost six times greater than that determined for the beam data. As β is the slope of the attenuation curve for X small, this result demonstrates the high-resolution capability of the mixed signal processor over that of the beam.

Solutions to equation (5) provide considerably better fits to the data than do those solutions based on equation (4). We therefore recommended employing the more generalized solutions in determining the number of opportunities for masking the signals from an explosion in the coda of an earthquake. When computing the number of opportunities, a given number of stations in a worldwide monitoring network would be given coda suppression capabilities based on the number of sensor elements specified (7 or 19) and the type of array processing to be performed (beam or mixed-signal processor). That is, a given station would be assigned one of the coda suppression curves listed in Table V.

TABLE V

Coda Attenuation Parameters

$$\rho = \frac{\beta X + \gamma X^2}{1 + \delta X + \varepsilon X^2}$$

where $X \equiv \delta\left(\frac{dT}{d\Delta}\right)$

19-ELEMENT SUBARRAY

BEAM	MIXED-SIGNAL PROCESSOR
0.98	5.74
0.14	0.91
0	0.31
0.006	0.43

7-ELEMENT SUBARRAY

BEAM	MIXED-SIGNAL PROCESSOR
0.37	2.21
0.04	0.69
0.00	0.53
0.00	0.005

An attenuation factor based on the vector difference in the ray parameters for the two epicenters under investigation can then be determined, and the coda of the masking earthquake scaled accordingly.

As a final note, let us compare the coda attenuation obtained for a wide-aperture 7-element TFO subarray (Z1, Z9, Z11, Z13, Z15, Z17, and Z19) with that obtained previously for the 19-element and small aperture 7-element subarrays (Table VI, Figures 31 and 32) The data analyzed are from the Easter Island event. For the wide-aperture 7-element subarray and with the exception of those azimuths for which the difference in the ray parameters is small, the beam and mixed-signal processor perform about equally well; the mixed-signal processor yields only 1 to 2 db additional attenuation over the beam. Further, the coda attenuation obtained using the wide-aperture 7-element subarray and the mixed-signal processor is about the same as that obtained for all 19-elements and the beam, as well as that obtained for the 7 inner elements (Z1-Z7) and the mixed-signal processor. Finally, for small ray-parameter separation, the wide-aperture 7-element subarray and the mixed-signal processor produce about the same attenuation as does the 19-element subarray and the mixed-signal processor (~9 db).

In sum, a wide aperture array and the mixed-signal processor are more important than the number of elements for significant coda attenuation when the difference in the ray parameters is small. When the ray parameter

TABLE VI

Comparison of Coda Attenuation Capabilities
Source Region: Semipalatinsk

SUBARRAY	PROCESSOR	AZIMUTH			
		0°	90°	180°	270°
		Attenuation in db			
7-element, small aperture	beam	0.6	5.4	9.5	4.1
7-element, small aperture	mixed-signal	1.9	15.6	13.4	5.6
7-element, wide aperture	beam	1.5	11.0	15.0	5.7
7-element, wide aperture	mixed-signal	8.4	12.9	15.1	6.7
19-element	beam	1.6	13.0	15.6	10.3
19-element	mixed-signal	9.6	15.7	17.3	15.4

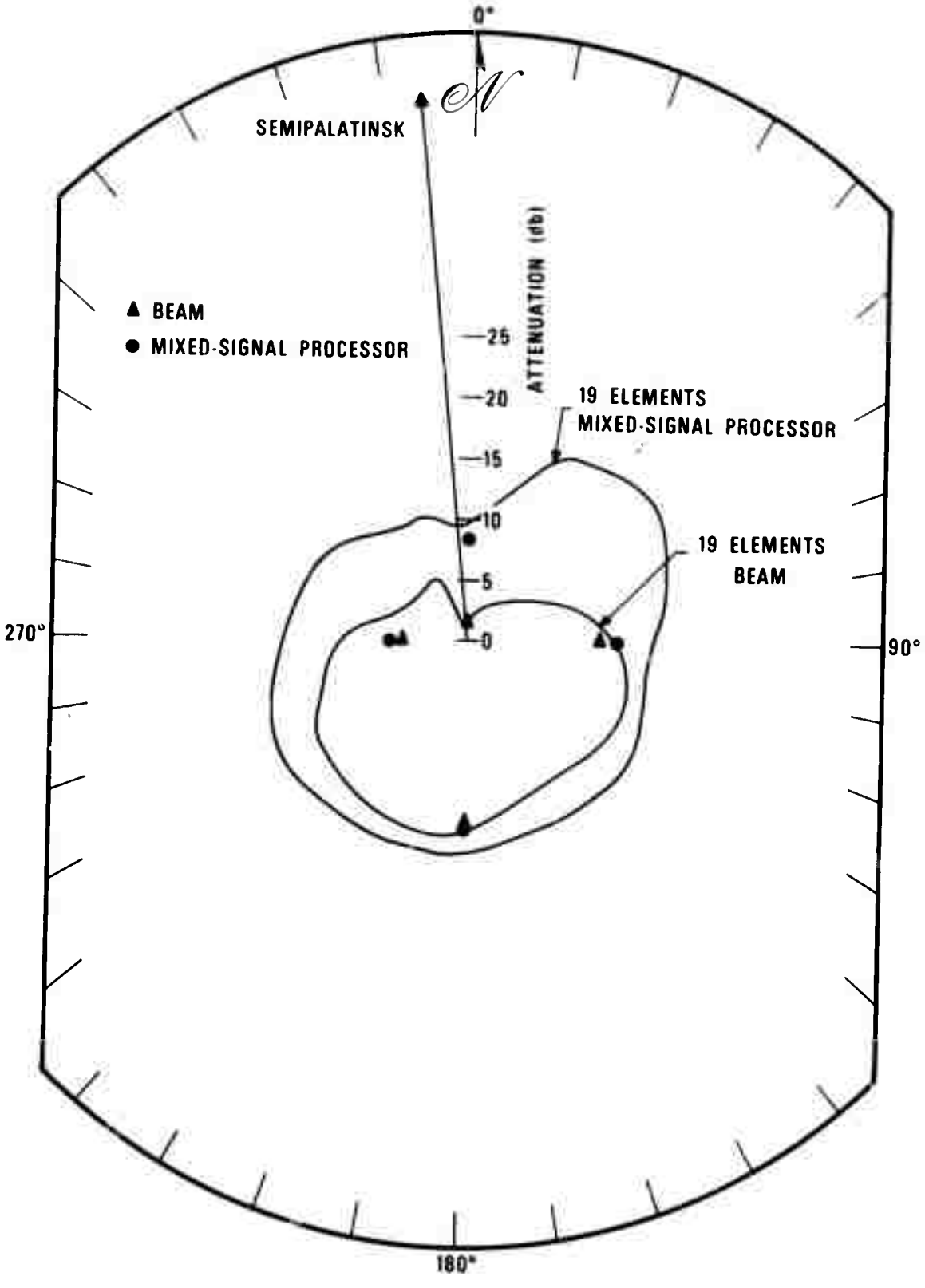

Figure 31. Comparison of coda attenuation figures, Easter Island event, 19-element subarray and wide-aperture 7-element array.

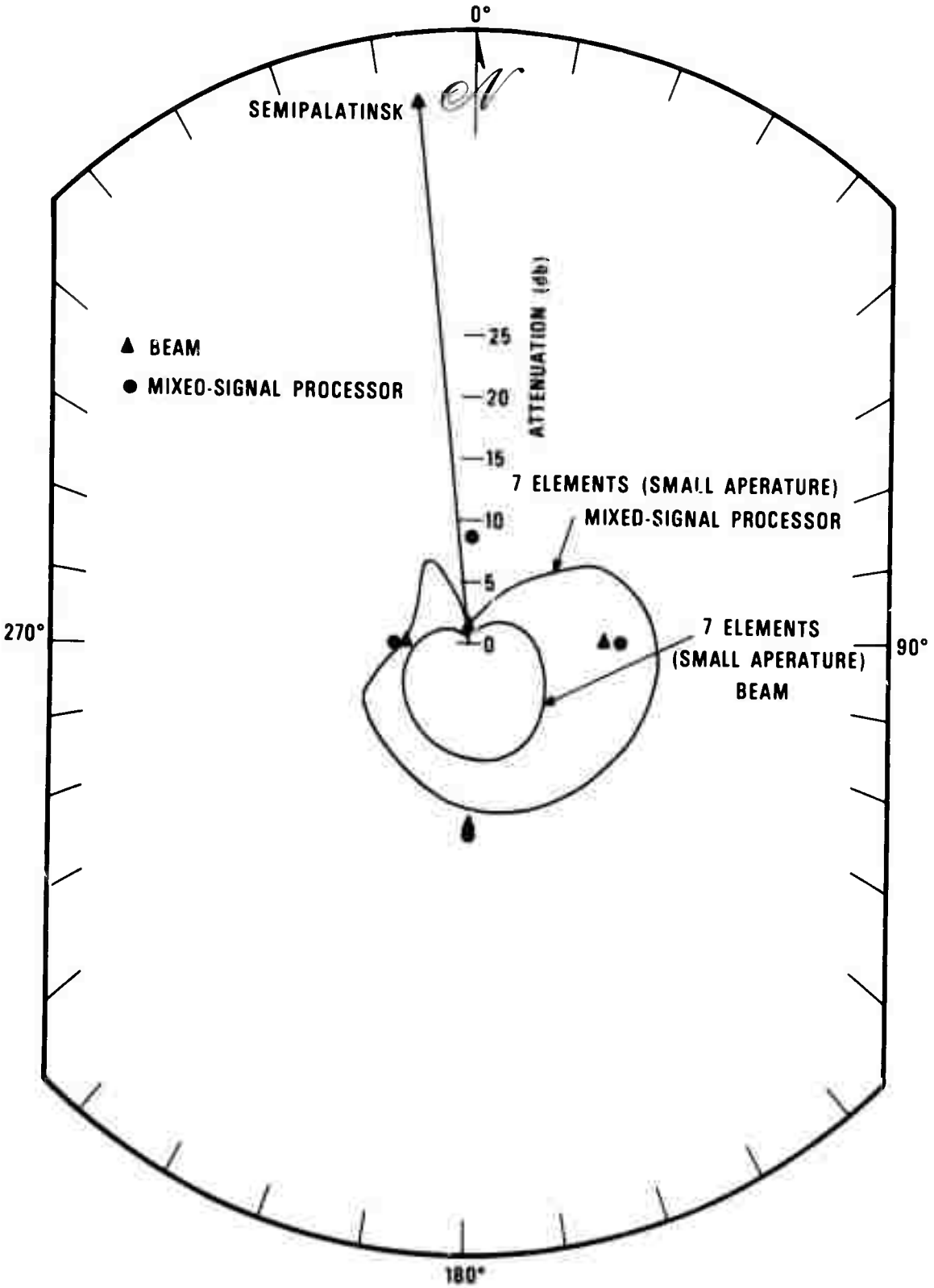

Figure 32. Comparison of coda attenuation figures, Easter Island event, small-aperture 7-element subarray and wide-aperture 7-element subarray.

difference is large, and when using the mixed-signal processor, the wide-aperture 7-element subarray performs about as well as the small-aperture 7-element subarray. Where using the beam, however, the wide-aperture 7-element subarray performs substantially better than does the small-aperture 7-element subarray, the improvement being on the order of 5 db.

CONCLUSIONS

A comparison has been made of the coda attenuation capabilities of the beam and mixed-signal processor using 7- and 19-element TFO subarrays. The major source region was taken as Semipalatinsk (96° distance from TFO), while the interfering signals from various earthquakes were time-shifted to simulate arrivals from various azimuths at 60° distance. Our major conclusions are:

1. The coda attenuation capability of the mixed-signal processor exceeds that of the beam. While up to 14 db improvement was obtained, the improvement is generally on the order of 3 to 5 db for both subarrays.

2. A nominal value of 18 db is representative of the maximum coda attenuation obtained using the mixed-signal processor and the 19-element array. For the 7-element array, the corresponding figure is 14 db.

3. The coda attenuation obtained using the 7-element subarray and the mixed-signal processor is comparable to that obtained using the 19-element array and the beam.

4. No advantage was observed in using data filtered in the band 0.8 to 2.0 Hz over that data which was filtered in the band 0.4 to 3.0 Hz.

5. Representative TFO coda attenuation curves for the mixed-signal processor are:

19 elements:

$$\rho = \frac{5.74X + 0.91X^2}{1 + 0.31X + 0.043X^2} \quad \text{db}$$

7 elements:

$$\rho = \frac{2.21X + 0.69X^2}{1 + 0.53X + 0.005X^2} \quad \text{db}$$

where

$$X \equiv \left| \left(\frac{d\vec{T}}{d\Delta}\right)_1 - \left(\frac{d\vec{T}}{d\Delta}\right)_2 \right|$$

6. For X small, the mixed-signal processor is six times more sensitive to changes in X than is the beam.

7. Preliminary investigations at TFO using a wide-aperture 7-element array suggest that for small differences in the ray-parameter vectors, a large-aperture array and the mixed-signal processor are more important than the number of elements for significant coda attenuation (~9 db).

REFERENCES

Dean, W.C., Shumway, R.H. and Duris, C.S., 1968, Best linear unbiased estimation for multivariate stationary processes: Seismic Data Laboratory Report No. 207, Teledyne Geotech, Alexandria, Virginia.

Shumway, R.H., 1972, Some applications of a mixed signal processor: Seismic Data Laboratory Report No. 280, Teledyne Geotech, Alexandria, Virginia.

ACKNOWLEDGEMENTS

The author is grateful to R.H. Shumway and R.R. Blandford for many helpful discussions on mixed-signal processing, and for their critical reading of the manuscript. T.J. Dutterer assisted in performing many of the computations.